

STRUCTURAL CONSTITUTIVE MODELS FOR KNEE LIGAMENTS

by

Raffaella De Vita

Laurea, University of Naples II, 2000

M.S., University of Pittsburgh, 2003

Submitted to the Graduate Faculty of
School of Engineering in partial fulfillment
of the requirements for the degree of
Doctor of Philosophy

University of Pittsburgh

2005

UNIVERSITY OF PITTSBURGH

SCHOOL OF ENGINEERING

This dissertation was presented

by

Raffaella De Vita

It was defended on

April 8, 2005

and approved by

Giovanni P. Galdi, Professor, Mechanical Engineering Dept.

Anne M. Robertson, Associate Professor, Mechanical Engineering Dept.

Michael S. Sacks, Professor, Bioengineering Dept.

Dissertation Director: William S. Slaughter, Associate Professor, Mechanical Engineering
Dept.

ABSTRACT

STRUCTURAL CONSTITUTIVE MODELS FOR KNEE LIGAMENTS

Raffaella De Vita, Ph.D.

University of Pittsburgh, 2005

It has been estimated that approximately 375,000 people experience knee injuries every year in the United States. The majority of the pathologies affect the anterior cruciate ligament (ACL) and the medial collateral ligament (MCL). Thus, a thorough characterization of the mechanical properties of the ligaments is needed to understand the etiology of their injuries and to improve the strategies of their treatment. The first chapter of this dissertation offers a brief overview of the morphology and mechanics of the ligaments.

Since injuries are estimated to occur at strain rates that range from 50%/s to 150,000%/s, studying the mechanical behavior of ligaments at various strain rates is imperative. In the second chapter, a structural constitutive model is formulated by taking into account the non-linearity, anisotropy, incompressibility, and strain rate-related properties of the ligaments. The collagen fibers, which comprise the ligament, are assumed to be the only load-bearing component of the tissue. They are oriented in various directions, undulated in the stress-free configuration, and they gradually become straight upon deformation. Moreover, the collagen fibers are characterized by a Kelvin-Voigt-type viscoelastic behavior. The fiber spatial orientation and gradual recruitment are represented statistically by probability density functions. Published experimental data on the ACLs are used to assess the constitutive model.

The most severe of the knee ligament injuries are partial and complete tears. Thus, there is a compelling need to understand the mechanical failure behavior of ligaments. In the third chapter, a structural constitutive model for the description of the ligament tensile properties is proposed. The model reproduces the three-regions of the nonlinear stress-strain relationship of ligaments. The collagen fibers contribute to the overall tissue's response after becoming taut and before failing and they are assumed to behave as a linear elastic material. The fiber recruitment and failure processes are stochastically defined. Available experimental data for the MCLs are employed to validate the constitutive relation. Furthermore, the generalization to a three-dimensional model is also given.

Future research directions toward the development of a structural constitutive model for the subfailure behavior of ligaments are indicated in the fourth chapter and conclusions are drawn in the fifth chapter.

TABLE OF CONTENTS

| | |
|--|-----|
| ABSTRACT | iii |
| LIST OF FIGURES | vii |
| ACKNOWLEDGMENTS | ix |
| 1.0 INTRODUCTION | 1 |
| 1.1 MOTIVATION | 1 |
| 1.2 LIGAMENT MORPHOLOGY | 4 |
| 1.3 LIGAMENT MECHANICS | 8 |
| 1.3.1 Quasi-Static Mechanical Properties | 8 |
| 1.3.2 Viscoelastic Mechanical Properties | 10 |
| 1.4 CONSTITUTIVE MODELS | 14 |
| 1.4.1 Structural Constitutive Models | 14 |
| 2.0 A STRUCTURAL MODEL FOR THE STRAIN RATE DEPENDENT BEHA- VIOR | 19 |
| 2.1 STRAIN RATE DEPENDENT BEHAVIOR OF KNEE LIGAMENTS | 19 |
| 2.2 MODEL FORMULATION | 23 |
| 2.2.1 Constitutive Equation | 23 |
| 2.2.2 Recruitment Model | 25 |
| 2.2.3 Fiber Elastic and Viscous Stresses | 26 |
| 2.3 MODEL IMPLEMENTATION | 28 |
| 2.3.1 Isochoric, Axisymmetric Deformation | 28 |
| 2.3.2 Collagen Fiber Orientation and Crimp | 28 |
| 2.4 RESULTS | 30 |

| | | |
|-------|--|----|
| 2.5 | DISCUSSION | 34 |
| 3.0 | A STRUCTURAL MODEL FOR THE FAILURE BEHAVIOR | 38 |
| 3.1 | FAILURE BEHAVIOR OF KNEE LIGAMENTS | 38 |
| 3.2 | MODEL FORMULATION | 41 |
| 3.2.1 | Recruitment and Failure Model | 42 |
| 3.2.2 | Model Generalization | 43 |
| 3.3 | RESULTS | 45 |
| 3.4 | DISCUSSION | 52 |
| 4.0 | FUTURE DIRECTIONS: A STRUCTURAL MODEL FOR THE SUBFAILURE DAMAGE | 55 |
| 4.1 | SUBFAILURE DAMAGE IN KNEE LIGAMENTS | 55 |
| 4.2 | MODEL FORMULATION | 57 |
| 4.3 | PRELIMINARY RESULTS | 59 |
| 4.4 | DISCUSSION | 62 |
| 5.0 | CONCLUSIONS | 64 |
| | BIBLIOGRAPHY | 67 |

LIST OF FIGURES

| | | |
|-------------|--|----|
| Figure 1.1 | Knee ligaments | 2 |
| Figure 1.2 | Hierarchical structure of collagen | 4 |
| Figure 1.3 | Quarter-stagger arrangement of tropocollagen in fibril | 5 |
| Figure 1.4 | Typical ligament stress-strain relationship | 7 |
| Figure 1.5 | Rat MCL collagen fibers waviness observed by scanning electron microscopy. The fibers appear to be wavy in the slack configuration (A), (B). They are observed to become straight in the reference configuration, under a 0.05 N load (C). When they are subjected to a 5 N load, they show to lose their waviness | 7 |
| Figure 1.6 | Ligament hysteresis and preconditioning effects | 11 |
| Figure 1.7 | Ligament stress-strain relationship at increasing strain rates | 12 |
| Figure 1.8 | Ligament creep (top) and relaxation (bottom) | 13 |
| Figure 1.9 | Nonlinear elastic model proposed by Frisen et al. Δ_i denotes the displacement of the fibril i , X denotes the displacement of the tissue and F denotes the force acting on the tissue | 15 |
| Figure 1.10 | Fiber orientation and undulation in a representative volume according to Lanir's model. \mathbf{M}_1 and \mathbf{M}_2 represent two of the many possible fiber material directions. Note that fibers are crimped differently along each material direction | 16 |
| Figure 2.1 | Assumptions in the recruitment model | 25 |
| Figure 2.2 | Λ : axial fiber stretch, Λ_s : straightening stretch | 26 |
| Figure 2.3 | Reference configuration (right) and current configuration (left) | 29 |

| | | |
|------------|---|----|
| Figure 2.4 | Stress-strain experimental data from Danto and Woo at 1.68%/s and 381%/s strain rates with model (—) and fraction of straight fibers (—) evaluated at best fitting parameters | 31 |
| Figure 2.5 | Experimental data from Pioletti and co-authors at 5%/s, 10%/s, 20%/s, 30%/s, and 40%/s strain rates (various symbols) and theoretical stress-strain curves (continuous line) | 32 |
| Figure 2.6 | Linear dependence of the sensitivity coefficients | 33 |
| Figure 3.1 | Λ_s : straightening fiber stretch, Λ_f : failure fiber stretch | 41 |
| Figure 3.2 | Assumption of the recruitment model with failure | 43 |
| Figure 3.3 | Stress-strain experimental data from Abramowitch and colleagues (●) with model fit (—), fractions of straight fibers (—), and fractions of broken fibers (—) | 48 |
| Figure 3.4 | Stress-strain experimental data from Abramowitch and co-authors (●) with five parameter model fit (—) and four parameter model fit (—) | 49 |
| Figure 3.5 | Stress-strain experimental data from Provenzano et al. (●) with model fit (—), fractions of straight fibers (—), and fractions of broken fibers (—) | 50 |
| Figure 3.6 | Stress-strain experimental data from Provenzano et al. (●) with five parameter model fit (—) and four parameter model fit (—) | 51 |
| Figure 4.1 | Λ_s : straightening fiber stretch. Λ_d : damage fiber stretch. Λ_f : failure fiber stretch | 58 |
| Figure 4.2 | Fiber stress-stretch relation | 59 |
| Figure 4.3 | Stress-stretch curves for the control rat MCL (●) and for the re-stretched rat MCL after the peak subfailure stretch $\Lambda_p = 1.09$. Model fit (—) and model prediction (—) are represented at best fitting parameters | 61 |

ACKNOWLEDGMENTS

I thank everyone who has taught me, inspired me, and supported me through my graduate studies at University of Pittsburgh.

First and foremost, I would like to thank my adviser, Prof. William S. Slaughter, for his guidance and mentorship over these years at University of Pittsburgh. It has been a great privilege to work with an outstanding teacher as him. He has taught me a lot in each of his lectures and in each of our research meetings.

I am very thankful to Prof. Michael S. Sacks for showing me the realm of Biomechanics. I especially thank him for the valuable discussions on structural constitutive models for soft tissues. After each of our discussions, I felt that I was working on a beautiful subject worthy of all my efforts. Special thanks are also extended to the members of the Engineered Tissue Mechanics Laboratory.

I would like to express my gratitude to Prof. Giovanni P. Galdi and Prof. Anne M. Robertson. They have played a significant role in my choice to pursue my graduate studies at University of Pittsburgh. I deeply thank them not only for all they have taught me but also for their warm hospitality and encouragement.

I thank Prof. Daniel Budny for whom I was teaching assistant for three years. He has made my teaching experience extremely enjoyable. Furthermore, I thank all the students who I had the privilege to teach and from whom I learnt.

Thanks to all my friends: Gaetano Sterlacci, Stefano Sacrato, Andrea La Gioa, Rachmadian Wulandana, Ana Silvestre, Fernando Carapau, Roxana Cisloiu, Brian Ennis, Shadow Huang, and Sandy Hu. My deepest thanks go to Ashwin Vaidya for his sincere friendship.

I express my gratitude to the staff of the Mechanical Engineering Department. I am especially grateful to the graduate administrator, Glinda Harvey, for her enormous help.

I would like to thank Prof. Remigio Russo and Prof. Giulio Starita for introducing me the subject of Mechanics during my undergraduate studies at University of Naples II.

Last but not least, I thank my family for their constant support. In particular, I thank my husband, Traian Iliescu, for his endless encouragement throughout my graduate studies.

Funding for this research was provided by NSF grant no. BES-9978858 and by the Graduate School of the Department of Mechanical Engineering, University of Pittsburgh. Supplemental funding was obtained by a research grant from the Department of Mathematics, University of Naples II, Caserta, Italy.

Let theory suggest experiments to perform; nothing could be better. Once the experimentation has been made and the results have been clearly observed, let theory take hold of them to generalize them, coordinate them, and draw from them new subjects of experiments; again nothing could be better.

(Duhem, 1861-1916)

1.0 INTRODUCTION

1.1 MOTIVATION

Ligaments are bands of fibrous tissue that transmit loads between bones and support internal organs. Their main function is to guide and to restrain joint motion in order to maintain joint stability. Among the ligaments of the human body, the ligaments of the knee joint have been extensively studied by the biomechanics community due to the joint's elevated vulnerability. Epidemiological research has indicated that approximately 375,000 people are affected by knee injuries every year in the United States. Particularly, ligament injuries are the most common, representing 40% of the knee problems.^{(1)*}

The major ligaments of the knee are the medial collateral ligament (MCL), the lateral collateral ligament (LCL), the anterior cruciate ligament (ACL), and the posterior cruciate ligament (PCL) (See Figure 1.1). The MCL and LCL span the femur and the tibia and they are situated on the inside and outside of the knee, respectively. The MCL's primary function is to limit the inward motion of the knee whereas the LCL fetters its outward motion. The ACL and PCL also run from the femur to the tibia but they are located and crisscross each other in the center of the knee. They restrain the forward and backward motion of the tibia, respectively.

The ACL and the MCL will be the focus of the present study since they are the most prone to injuries. Indeed, recent studies reported that 46% of the ligamentous problems involve the ACL, 29% affect the MCL, and 13% consist of combined ACL-MCL pathologies.⁽¹⁾ These injuries occur mostly during sport activities such as skiing, basketball, football, and soccer and are caused by planting, cutting, pivoting, and tackling maneuvers.

*Parenthetical references placed superior to the line of text refer to the bibliography.

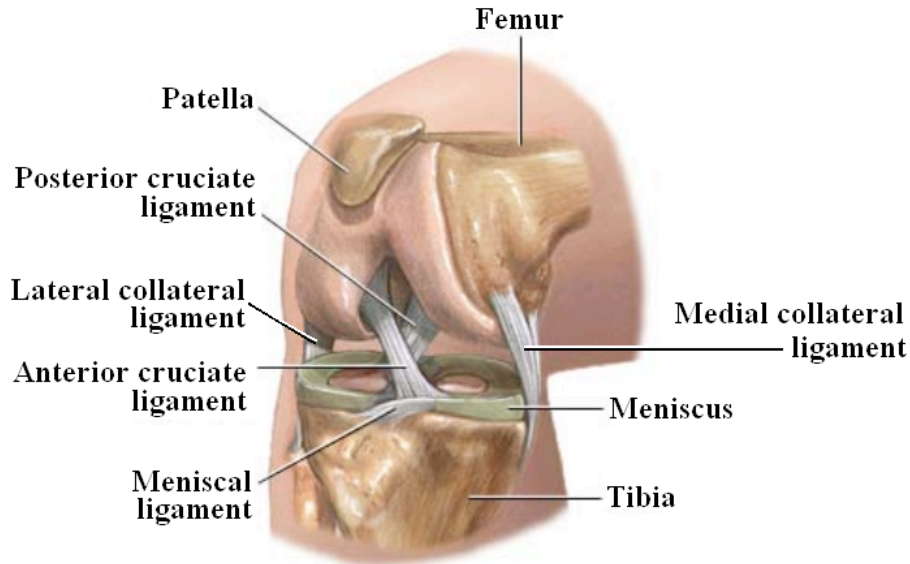


Figure 1.1. Knee ligaments.⁽²⁾

Injuries to the ligaments can be classified according to their severity as first-degree sprain, second-degree sprain and third-degree sprain. With a first-degree sprain, the ligament is overstretched but the joint remains stable. A second-degree sprain occurs when the ligament is partially torn and it moderately affects the joint stability. A third-degree sprain is the most debilitating ligament injury. It consists of a complete rupture of the ligament and it causes severe joint instability. The medical treatment varies with the degree of injury from the simple RICE (rest, ice, compression, elevation) rule to graft implantation.

The choice between conservative treatment with no repair and surgical treatment with repair of the torn MCLs and ACLs remains controversial among orthopedists. The MCL rupture usually heals spontaneously. However, without a surgical repair, disorganized scar tissue fills the gap between the torn ends of the MCL and the knee presents some instabilities. On the contrary, the ACL acute tear often requires surgical intervention due to the ligament's poor healing properties and limited vascularization. A non-operative treatment of ACL tear can lead to gross instabilities of the knee and, hence, it can seriously compromise the physical activity of the patients.

Several kinds of ligament grafts are utilized for knee ligament reconstruction when complete tear occur.⁽³⁾ Orthopedic surgeons most commonly use autografts, grafts harvested from the patients. The autografts are obtained from the middle-third of the patellar tendon, from one or two hamstring tendons, and from the distal portion of the iliotibial tract. Allografts represent the other grafts of choice in knee ligament surgery. The source material of these grafts is mainly derived from human donor hamstring tendons, patellar tendons, and Achilles tendons. Although xenografts, which are grafts harvested from an animal donor, and synthetic polymer grafts have been employed for ligament reconstruction, they are not recommended for reconstructive surgery due to their short-term durability and poor biocompatibility. In recent years, fibroblast seeded collagen matrix, fibroblast seeded polymer scaffolds and growth factors that enhance the healing of ligament injuries have shown promising success in ligament tissue engineering.⁽⁴⁾

In order to reduce the incidence of the ACL and MCL injuries, to understand their mechanisms, to improve their strategy of treatment, and to construct improved ligament graft substitutes, a thorough study of the mechanical properties of these tissues is required. Enormous advances have been made in experimental mechanics to accurately characterize the biomechanics of ligamentous tissues. The majority of experimentalists investigated the uniaxial properties of the ligaments and performed their measurement by assuming the tissue to be homogenous. However, during the knee joint activity these ligaments are subjected to three-dimensional deformations that are combinations of tension, compression, shear, bending, and torsion. Moreover, the ligaments exhibit inhomogeneities, which are pronounced at the bone insertions.⁽⁵⁾

Experimental difficulties and limitations call for the need of an adequate constitutive theory that can enhance the understanding of the complex mechanical behavior of the ligamentous tissue. Constitutive models can guide the design of suitable experiments and describe mechanical features of the tissue that are impossible to capture solely by means of experimental investigations. As noted by Truesdell,⁽⁶⁾

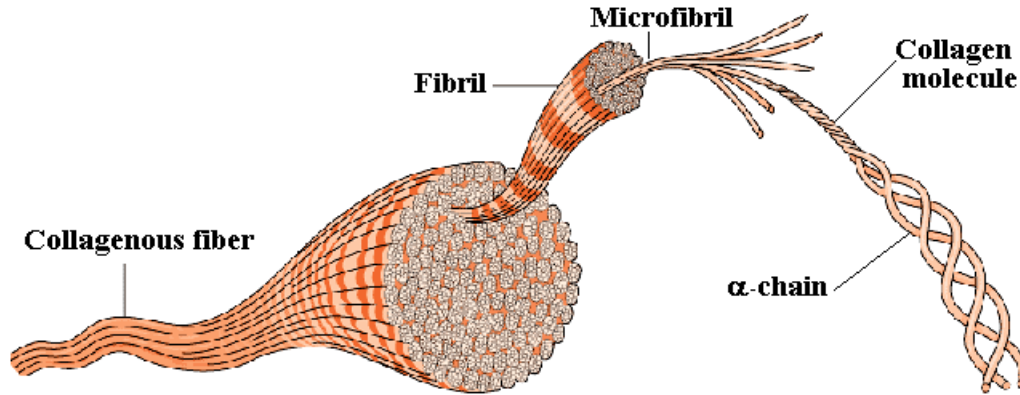


Figure 1.2. Hierarchical structure of collagen.⁽⁷⁾

Of course, physical theory must be based on experience, but experiment comes after, not before, theory. Without theoretical concepts one would neither know what experiments to perform nor be able to interpret their outcome.

This study aims at formulating *structural* constitutive relationships for the short-time memory dependent behavior and the mechanical failure of knee ligaments. Unlike *phenomenological* models, these constitutive models are formulated by taking into account the tissue components, their geometry and their interactions. Thus, in this chapter, the morphological and mechanical properties of the ligaments, which are significant to the development and to the discussion of the proposed constitutive models, will be reviewed.

1.2 LIGAMENT MORPHOLOGY

Ligaments are connective tissues that consist of collagen and elastin embedded in a ground substance of water, proteoglycans, glycolipids, and fibroblasts. Collagen is the main load carrying component in ligamentous tissues. It is the most abundant protein constituting 65% – 80% of the ligament dry weight.⁽⁸⁾ In parallel-fibered tissues, such as ligament and tendon, collagen is characterized by a hierarchal structure: collagen molecules are packed together to form collagen fibrils, collagen fibrils aggregate to form collagen fibers and collagen

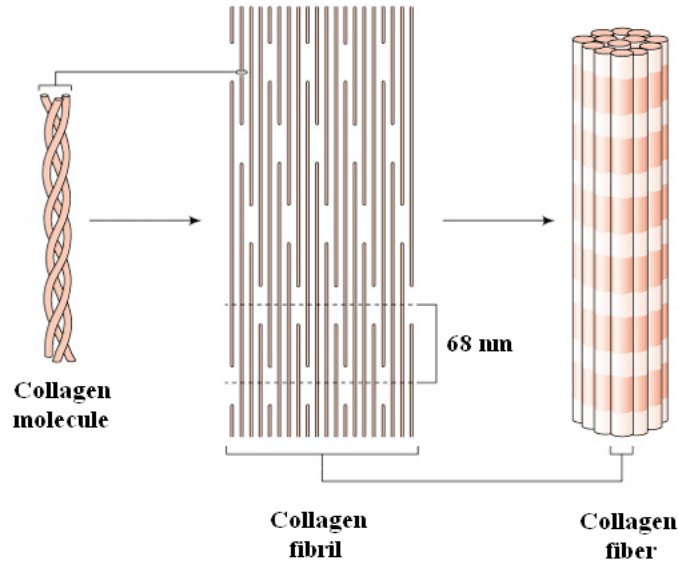


Figure 1.3. Quarter-stagger arrangement of tropocollagen in fibril.⁽⁷⁾

fibers are arranged in fascicles that run parallel to the ligament loading direction (See Figure 1.2). The collagen molecule, also known as tropocollagen, possesses a right-handed triple helix structure formed by chains of amino acids. The amino acid chains, called α -chains, in turn, have a left-handed helical conformation. In particular, each α -chain is composed of sequences of glycine-x-y where x and y are common amino acids, mainly proline and hydroxiproline, stabilized by hydrogen bonds.

More than 15 types of collagen molecules have been identified. Type I collagen is the main ligament fiber-forming molecule. It is composed by two $\alpha 1(I)$ chains and by one $\alpha 2(I)$ chain, which have specific amino acid sequences.⁽⁹⁾ Collagen type III, another fiber-forming molecule, and collagen type IV are also found in the ligament sheaths.⁽¹⁰⁾

Groups of four or five collagen molecules are arranged in a quarter-stagger fashion to form a microfibril. The microfibril striation, which is observed in the electron microscope, has a period D of 68 nm. Each collagen molecule has a length of 4.4D with a 0.4D overlapping region. The gap region between neighboring molecules is 0.6D. Subsequently, microfibrils are assembled into fibrils and fibrils into fibers (See Figure 1.3).

The collagen fibers appear to be wavy when the ligamentous tissue is unloaded. There is no agreement among investigators in biomechanics on the fiber waveform. It is described as helical by Comninou and Yannas,⁽¹¹⁾ planar sinusoidal by Diamant et al.⁽¹²⁾ and planar zig-zag by Kastelic et al.⁽¹³⁾

Elastin is the other significant protein in ligamentous tissue. It constitutes less than %1 of the tissue dry weight and it is found in the walls of the blood vessels. It is responsible for the elastic recovery of these tissues. Exceptionally, ligamentum nuchae, which joins the skull to the neck, and ligamenta flava, which connect the laminae of adjacent vertebrae, are primarily made of elastin.

Collagen and elastin are embedded in an amorphous ground substance or gel matrix. The ligament ground substance is comprised of water, proteoglycans, and glycoproteins. Water occupies 60 – 70% of the tissue total weight.⁽⁸⁾ Proteoglycans consists of core proteins with multiple covalently attached glycosaminoglycans. Because of their negative charge, these proteins exert repulsive forces amongst themselves and spread within collagen fibrils and fibers. Moreover, they possess hydroxyl groups that attract water through hydrogen binding. Their main function is to regulate the movement of water in the ground substance. Fibronectin and laminin are large glycoproteins that mediate the communication between the cells and the surrounding extracellular matrix. Particularly, fibronectins are responsible for anchoring fibroblasts to the collagen substrates and, therefore, they play significant roles during tissue growth, healing and remodeling. Laminin functions to bind collagen type IV to cell membranes. The cells, fibroblasts or fibrocytes, are rather sparse within the ligamentous tissues and they synthesize collagen.⁽¹⁰⁾

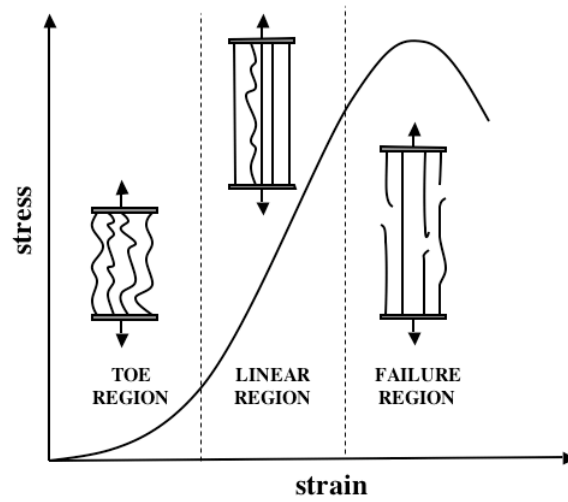


Figure 1.4. Typical ligament stress-strain relationship.

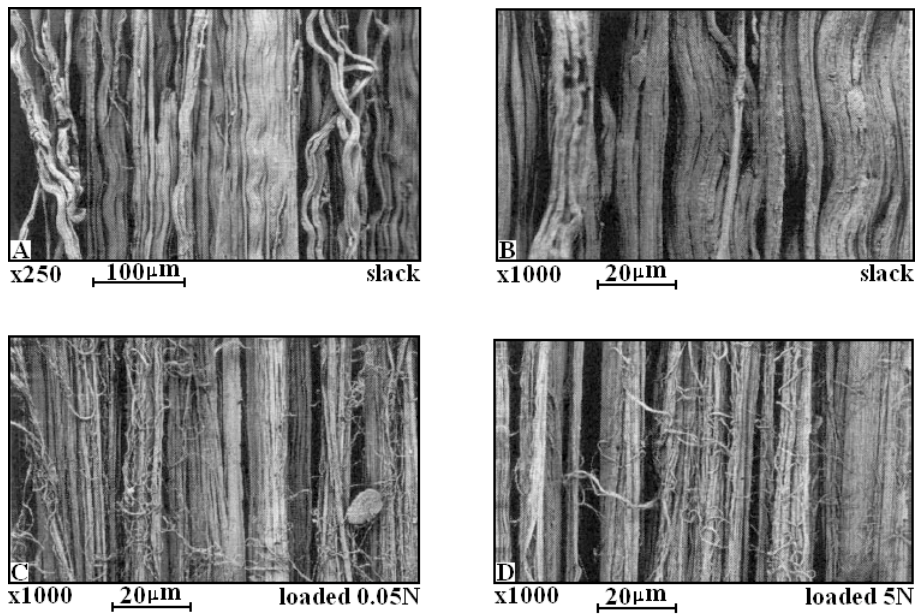


Figure 1.5. Rat MCL collagen fibers waviness observed by scanning electron microscopy. The fibers appear to be wavy in the slack configuration (A), (B). They are observed to become straight in the reference configuration, under a 0.05 N load (C). When they are subjected to a 5 N load, they show to lose their waviness.⁽¹⁴⁾

1.3 LIGAMENT MECHANICS

1.3.1 Quasi-Static Mechanical Properties

With few exceptions,^(15,16) tests to characterize the mechanical behavior of ligaments have been uniaxial tests along the ligaments' physiological loading direction. The material properties, described by stress-strain curves, are acquired by conducting these tests either on the ligament substance or on bone-ligament-bone complexes. Nevertheless, when the ligament-bone complexes are used, these properties are measured only when the ligament mid-substance fails without involving the failure of the bone.

The typical uniaxial stress-strain relationship for ligaments under quasi-static loading conditions is depicted in Figure 1.4. Like other soft connective tissues, the mechanical behavior of ligamentous tissue is nonlinear. Three regions can be individuated: the “toe” region, the linear region, and the failure region. These distinct parts of the stress-strain curve are correlated to the different structural changes occurring into the tissue during uniaxial loading.

Collagen fibers are mostly oriented in the direction of applied physiological stresses and they appear to be wavy in the slack configuration. Upon loading, the fibers lose their waviness and start to carry load. It is commonly believed that the gradual fiber straightening determines the toe region in the ligament stress-strain curve.^(14,17,18)

A number of investigators have analyzed the effects of crimp on the mechanical properties of collagen, utilizing polarized light microscopy, electron microscopy, x-ray diffraction techniques, and optical coherence tomography.^(12,13,17,18) Recently, Hurschler and co-workers⁽¹⁴⁾ conducted electron microscopic studies on rat MCLs and they demonstrated that the straightening of crimped fibers under load occurred both in normal and healing tissues. In Figure 1.5, results of their study for normal ligaments are shown.

Collagen fibers are considered to be responsible for the ligament stiffness and strength. As the load increases, the tissue is found to be less compliant. Moreover, the collagen fibers

straighten out and the mechanical response tends to become linear. At the failure region, perhaps collagen fibers start to break gradually until a complete tear of the ligament occurs. By using optical coherence tomography, Hansen et al.⁽¹⁸⁾ measured the changes in crimp during uniaxial extension of rat tail tendon fascicles. They noted that the crimp period increased with the axial strain and that the crimp bands extinguished when the stress-strain relation became linear.

Quantification of the tensile properties of ACL and MCL has received the attention of several researchers in biomechanics. Clearly, knowledge of tensile strength, ultimate strain and tangent modulus of these ligaments is essential for the prevention and treatment of injuries.

The ACL and the MCL mechanical properties have been compared by Woo et al.⁽¹⁹⁾ The authors reported that the tangent modulus of the MCL was twice that of the ACL in rabbits. By conducting scanning and transmission electron microscopic studies, the authors explained that this difference in the tangent modulus was due to the different collagen densities of the two ligament types. Collagen fibers were densely packed in the main axis direction of the ACL whereas, in the ACL, space among the fascicles of collagen fibers was observed. Furthermore, more collagen fibers were transversely oriented to the main axis in the ACL.

When conducting experiments by using non-contact strain techniques, Woo et al.⁽²⁰⁾ found the tangent modulus, the tensile strength, and the ultimate strain for the rabbit MCL to be approximately 740 MPa, 77.7 MPa, and 12.9%, respectively. By using similar experimental techniques, Quapp and Weiss⁽¹⁵⁾ determined the tangent modulus, the tensile strength, and the ultimate strain for human MCL to be approximately 332.2 MPa, 38.6 MPa, and 17.1%, respectively.

The skeletal maturity effects on the mechanical properties of the knee ligaments have also been examined.⁽¹⁹⁾ Different age groups of rabbits were used to study the changes in the tibia-MCL-femur tensile properties with maturity. Since failure occurred by tibia avulsion in

rabbits with open epiphyses,¹ the mechanical properties of the ligamentous substance could not be acquired. For rabbits with closed epiphyses, tearing in the ligament substance was the predominant mode of failure and the mechanical properties among these groups were found to be similar.

Uniaxial tests have been conducted on ligament substance along and transverse to the main collagen fiber direction.⁽¹⁵⁾ The resulting stress-strain curve for the ligament in the transverse direction appeared to be almost linear and the tensile strength, ultimate strain and tangent modulus were profoundly smaller than the corresponding longitudinal quantities.

The values of the tensile strength, ultimate strain, and tangent modulus vary with the ligament type, the animal specie, age and sex, the injury and treatment regime, and the experimental techniques. Therefore, one needs to be careful in comparing the different experimental results and in delineating the mechanics of the knee ligaments.

1.3.2 Viscoelastic Mechanical Properties

Ligaments display history and time dependent mechanical properties. The stress-strain curves described by these tissues during loading and unloading at a constant strain rate are different and give rise to hysteretic loops. Particularly, the unloading curve is shifted to the right. It has lower stress-strain slope at the low strain and higher stress-strain slope at higher strains than the loading curve (See Figure 1.6). Because of this hysteresis phenomenon, it is common practice to precondition the ligamentous tissue before acquiring the mechanical properties. Preconditioning is an experimental procedure in which the tissue is cyclically loaded and unloaded until the mechanical response becomes repeatable. This procedure has been shown to produce an increase in the reference length of collagenous tissues.⁽²¹⁻²³⁾

As a result of the short-time memory, the stress values of these tissues under dynamic uniaxial loadings is higher than those at equilibrium, for the same strain and, consequently,

¹*Epiphysis* is the end of a long bone that is initially separated from the main bone by a layer of cartilage and, subsequently, becomes united to the main bone through the ossification process.

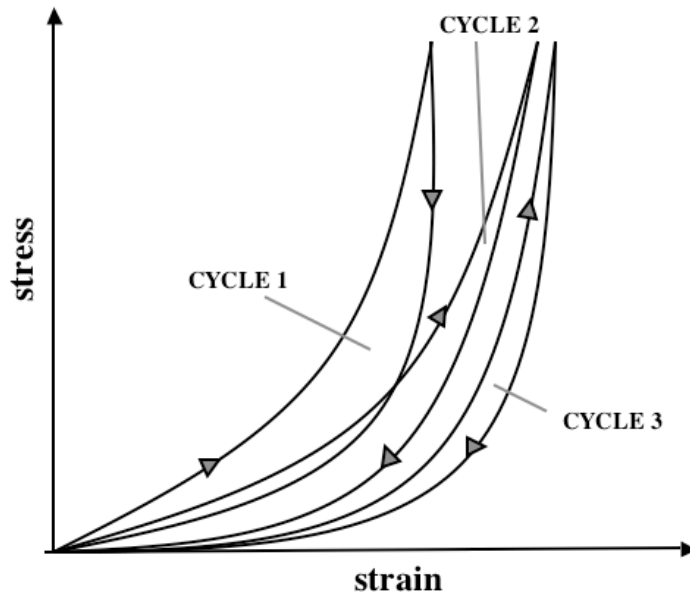


Figure 1.6. Ligament hysteresis and preconditioning effects.

the stress-strain curve appears to be ‘stiffer’ (See Figure 1.7). Few studies have analyzed the effects of strain rates on the mechanical properties of the knee ligaments.^(24–27) This scarcity is attributable to limitations of the experimental equipments in testing biological tissues at high ($> 1000\%/s$) strain rates.⁽²⁸⁾ These studies will be reviewed in detail in the next chapter since they lead to the formulation of a structural constitutive model and to their partial validation.

The long-time memory behavior of the tissues is manifested during diverse testing procedures.^(16,27,29–32) Several experiments on knee ligaments have shown that a continuous deformation of these tissues occurs when they are subjected to constant stress (creep) and a gradual decrease in stress with time occurs when they are under constant strain (relaxation) (See Figure 1.8). These tests have been mainly performed along the collagen fiber direction.⁽¹⁶⁾

Experimental work on ligamentous tissues has been mainly focused on stress relaxation tests. Some investigators have emphasized the need of studying the creep phenomenon of ligaments together with the relaxation phenomenon because ligaments are perhaps more

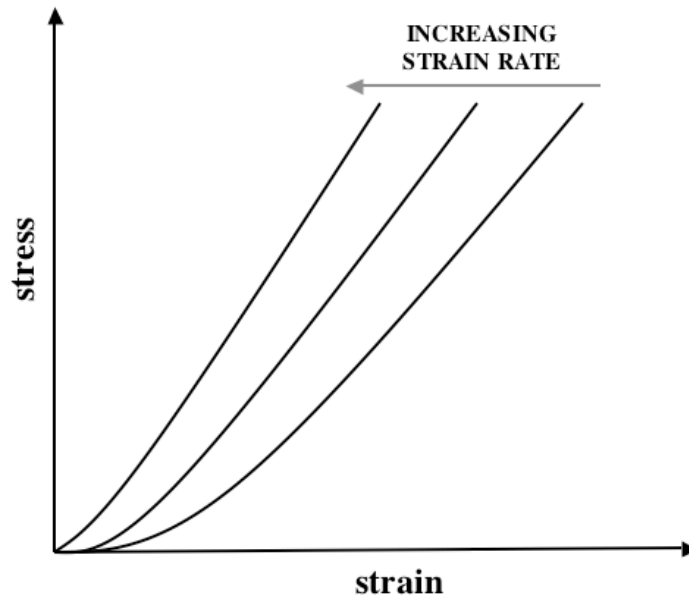


Figure 1.7. Ligament stress-strain relationship at increasing strain rates.

subjected to repeated stress than to repeated strain *in vivo*.⁽³¹⁾ Thornton and associates reported that creep in rabbit MCL is more nonlinear than relaxation. These findings were interpreted by considering the different structural changes occurring in the tissues during the two phenomena. In particular, collagen fibers are gradually recruited when the ligament is subjected to a constant load. Contrarily, they are recruited all at once when the ligament undergoes relaxation.⁽³¹⁾

Provenzano et al. performed creep and relaxation studies on rat MCLs at different loads and deformations below the damage threshold.⁽³²⁾ Their findings demonstrated that the rate of creep is stress dependent and the rate of relaxation is strain dependent. In particular, the rate of relaxation decreased with increasing strain and the rate of creep decreased with increasing stress. Moreover, relaxation was observed to proceed faster than creep, in agreement with other studies.⁽³¹⁾ These experimental observations proved the inadequacy of the quasi-linear viscoelastic theory, proposed by Fung,⁽⁹⁾ in capturing the ligament nonlinear viscoelastic behavior.

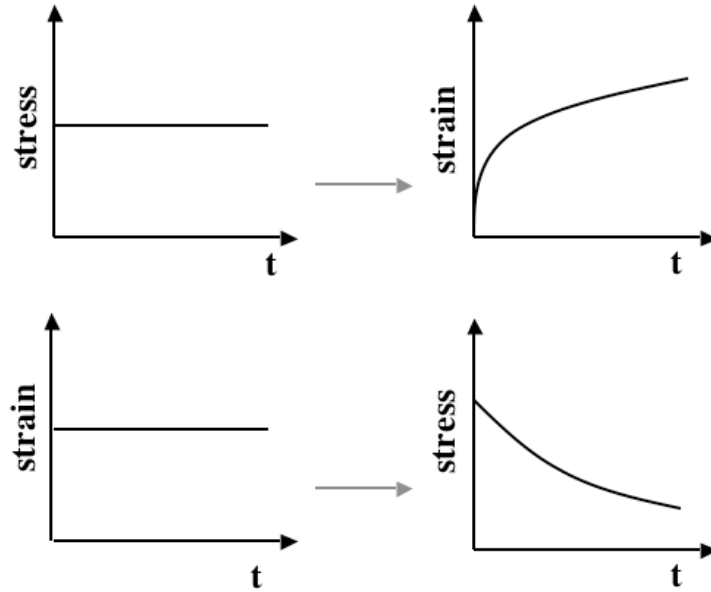


Figure 1.8. Ligament creep (top) and relaxation (bottom).

The source of the ligament viscoelasticity remains controversial. Minns et al.⁽³³⁾ have observed a decrease in relaxation and hysteresis when removing the fluid-like matrix from human tendon, human aorta, and bovine ligamentum nuchae with an enzyme or a chelating agent. These changes were explained by the decrease of the matrix viscosity in the tissues. Nevertheless, for the tendon, the inherent time-dependent behavior of collagen and the cross-linking among collagen fibrils, which is provided by the glycoproteins in the matrix, were also considered responsible. A recent study,⁽¹⁶⁾ in which the viscoelastic properties of human MCLs were investigated under longitudinal, transverse, and shear loadings, also suggested that the inter-fibrillar and/or inter-molecular cross-links contribute to the viscoelastic response of the ligaments. Moreover, because the increase in water content in immature rabbit MCLs has been shown to increase the relaxation,⁽³⁴⁾ some investigators attributed the viscoelasticity of the ligaments to the fluid in the ground substance. To date, the results of these studies are insufficient to draw conclusions on the role of the individual components on the overall tissue viscoelasticity.

1.4 CONSTITUTIVE MODELS

Constitutive relations are mathematical relationships that describe the mechanical behavior of materials under *specific* external conditions. It needs to be emphasized that constitutive equations describe behaviors not materials and they are valid only under certain conditions.

Theoretical understanding of ligament mechanics has advanced greatly in the past decades. Both phenomenological and structural constitutive relationships have been proposed for ligaments. Phenomenological models are derived directly from experimental observations of the gross mechanical behavior. Unlike phenomenological models, structural constitutive models are formulated by modeling the tissue's components, their geometry and their interactions. Therefore, the material parameters embodied in such models are directly related to the tissue's structure. However, complete descriptions of the tissues by such models require information about fiber orientation, fiber crimping, fiber volume fraction, and interaction among constituents, which are difficult to acquire.

In this study, *the structural approach is preferred to the phenomenological one* since it helps to elucidate the role of individual components in the gross mechanical response of the tissue. By following this approach, the study aims at formulating three-dimensional constitutive relationships to describe the short-time memory behavior and the failure behavior of ligaments. A review of structural and phenomenological constitutive laws proposed for the description of these behaviors for collagenous material will be presented in the next chapters. Hereafter, the general structural framework, which leads to the formulation of these models, will be presented.

1.4.1 Structural Constitutive Models

The first mathematical model that captured the structural changes occurring in soft biological tissues under uniaxial loading was proposed by Viidik et al.⁽¹⁷⁾ and improved by Frisen et al.⁽³⁵⁾ In these early works, soft collagenous tissues were modeled as composed of parallel

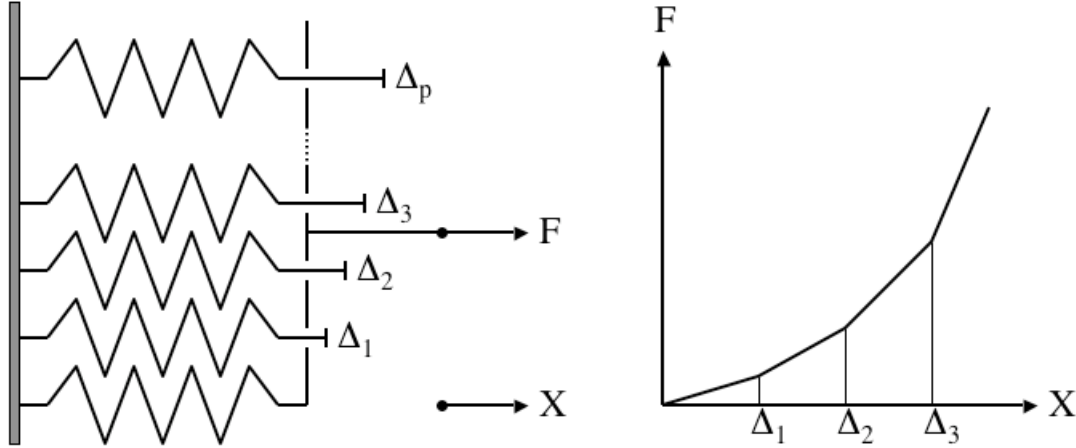


Figure 1.9. Nonlinear elastic model proposed by Frisen et al.⁽³⁵⁾ Δ_i denotes the displacement of the fibril i , X denotes the displacement of the tissue and F denotes the force acting on the tissue.

linear elastic fibrils that gradually become taut under load, bear load and, consequently, give rise to the typical nonlinear elastic behavior (See Figure 1.9).

Diamant et al.⁽¹²⁾ formulated a structural models for collagenous tissues in which the crimped fiber was idealized as a series of slender arms connected by elastic strings. Stouffer et al.⁽³⁶⁾ proposed a constitutive law for human patellar tendon that is based on similar ideas. By using a linearization of finite strain beam theory, Comninou and Yannas⁽¹¹⁾ developed a constitutive description for parallel-fibered tissues by assuming constant sinusoidal crimp for the collagen fibers. The crimp patterns of the fibers, which comprise the soft tissues, were assumed to be different in a one-dimensional model presented by Decraemer et al.⁽³⁷⁾ Particularly, the fiber straightening stretches are distributed according to a Gaussian distribution with a fixed mean.

Kastelic et al.⁽³⁸⁾ proposed the so-called SSL (sequential straightening loading) model which relates the fibril crimp morphology to the tensile properties of the collagen. In this model, the collagen fascicle was idealized as being composed of elastic fibrils with different crimp angles. The crimped fibrils offer no resistance to load and they sequentially become straight and support load. Stress-strain curves obtained from tensile tests on rat tail tendons

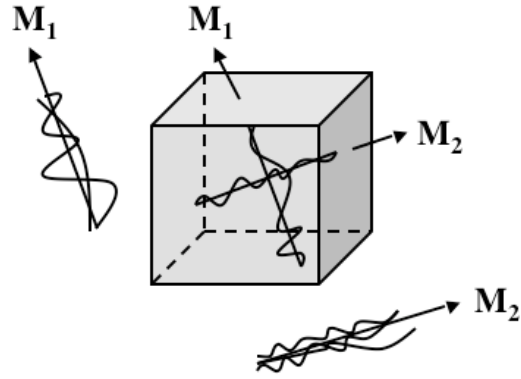


Figure 1.10. Fiber orientation and undulation in a representative volume according to Lanir's model.⁽⁴¹⁾ \mathbf{M}_1 and \mathbf{M}_2 represent two of the many possible fiber material directions. Note that fibers are crimped differently along each material direction.

of various ages were used to analyze the predictive capability of the model. By using different crimp angles, the toe region of the stress-strain curves was reproduced.

The structural three-dimensional constitutive theory for connective tissues developed by Lanir is pivotal for the formulation of the models that will be presented in the next two chapters.⁽³⁹⁻⁴¹⁾ According to Lanir's approach,⁽⁴¹⁾ the gross mechanical response of connective tissues is attributed to the mechanical properties and geometrical arrangement of the tissue's components: fiber families and ground substance. It is assumed that the strain energy of the tissue is the sum of the strain energies of individual fibers. Moreover, the fibers are oriented in different directions and have different undulations in the the tissue (See Figure 1.10). Both the fiber orientation and the fiber crimping are stochastically defined in a manner similar to Soong and Huang.⁽⁴²⁾ Since the load necessary to straighten the fiber is negligible, the fiber is assumed to support load only after losing the crimp. The mechanical behavior of the taut fiber is described as linear elastic or linear viscoelastic. Each fiber undergoes a uniaxial deformation, which is related to the gross tissue deformation by a tensorial transformation. The ground substance is assumed to sustain only hydrostatic pressure. For flat soft tissues,⁽³⁹⁾ Lanir assumed that the elastin and collagen fibers are responsible for the overall mechanical response at low strains and high strains, respectively.

Two versions of the constitutive theory were presented in order to account for the high and low densities of cross-links among fibers.⁽³⁹⁾ Lanir also proposed a constitutive model for the rheological model of tendons.⁽⁴⁰⁾ However, because of the lack of morphological information, the capabilities of the proposed models in simulating the mechanics of connective tissues were partially evaluated.

Lanir's constitutive law was adopted by Quapp and Weiss⁽¹⁵⁾ to describe the quasi-static mechanical behavior of human MCL under uniaxial loads, which were applied along and transverse to the collagen fiber directions. By assuming that all collagen fibers were oriented along the longitudinal direction, the constitutive model was found to be well suited to represent the mechanical response of ligaments, as observed in the experimental investigation. Because the ground substance was assumed to contribute to the total stress field of the tissue through a hydrostatic pressure, the transverse stress estimated by the model was zero. Nevertheless, the experimental findings demonstrated that, although the tensile material properties were significantly smaller in the transverse direction than in the longitudinal direction, they were not zero as the model predicted. The authors suggested that more experimental studies are needed to accurately assess the role of the tissue components and their interactions on the gross ligament mechanical behavior.

The structural models, originally proposed by Lanir, were successfully used to characterize the mechanical behavior of passive myocardium⁽⁴³⁾ and bioprosthetic heart valve.^(44–47) By using the small angle light scattering technique,⁽⁴⁸⁾ the collagen fiber orientation was quantified and incorporated in the constitutive models to describe the biaxial mechanical response of native and chemically-treated porcine and bovine pericardium by Billiar and Sacks⁽⁴⁵⁾ and Sacks.^(46,47) These studies demonstrated the utility of the structural approach in reducing the number of parameters to be determined and, consequently, the number of biaxial tests to be performed for the parameter estimation. Furthermore, the material parameters were physically meaningful and allowed to understand the relation between the tissue's structural architecture and overall mechanical behavior.

Despite the success of the above studies,^(45–47) the use of the structural theory for soft biological tissues is limited due to the difficulties in evaluating fiber waviness and fiber orientation distributions in non-planar tissues. Nevertheless, structural models remain helpful in investigating the relation between the morphology and the mechanics of biological tissue since they can describe behaviors which are difficult to capture by histological and mechanical investigations.

2.0 A STRUCTURAL MODEL FOR THE STRAIN RATE DEPENDENT BEHAVIOR

2.1 STRAIN RATE DEPENDENT BEHAVIOR OF KNEE LIGAMENTS

Injuries of the knee joint are estimated to occur at strain rates that range from 50%/s to 150,000%/s during sport activities and car accidents.⁽⁴⁹⁾ Therefore, examining the mechanical properties of knee ligaments under dynamic loading is essential in order to understand the mechanisms of these injuries. However, because experimental equipments are unable to record data at high speeds, the vast majority of researchers in biomechanics investigated the quasi-static mechanical response of the ligaments. Few experimental and theoretical studies have been devoted to analyzing the elongation or load rate dependent mechanical features of these tissues.

The highest strain rate, which has been used to characterize the mechanics of knee ligaments, is approximately 19,000%/s.⁽⁴⁹⁾ Crowninshield and Pope noted that, in clinical studies, the mode of failure of the knee ligaments was tearing whereas, in quasi-static experimental investigations, failure occurred by avulsion at the insertion sites of the ligaments to the bone. Thus, they carried out experimental studies in which the MCL-bone complexes were tested under quasi-static and dynamic loading conditions to elucidate the mechanisms of failure. By using a drop hammer device, traumatic loading rates of 19,000%/s and 51,000%/s were achieved. This study revealed that the mode of failure is strain rate dependent and that the ligament tearing becomes the predominant mode of failure at high strain rates. The tensile strength and the ultimate strain were observed to increase with strain rate. However, due to limitations in the testing apparatus, these mechanical properties could not be recorded at the 51,000%/s strain rate.

In 1990, skeletally immature and mature rabbit femur-MCL-tibia complexes were subjected to uniaxial loading at five extension rates that vary from 0.008 mm/s to 113 mm/s corresponding to 0.01%/s and 220%/s strain rates, respectively.⁽²⁴⁾ The linear stiffness, ultimate load, ultimate deformation, and energy absorbed at failure increased significantly with the elongation rate for the skeletally immature rabbits. Moreover, because the femur-MCL-tibia complexes for these rabbits were found to fail by tibial avulsion due to the skeletal maturation process, the mechanical properties of the ligaments could not be determined. For the group of mature animals, the authors found that tangent modulus, the tensile strength, and the ultimate strain increased with the strain rate. The femur-MCL-tibia samples failed by ligament tearing perhaps in virtue of the high strain rate dependency of bones. Woo and co-authors⁽²⁴⁾ concluded that the effects of strain rate on the material properties of the ligaments was not profound in the range of strain rates used in their study. Nevertheless, they recognized that the ligaments should be tested under higher strain rates ($> 1000\%/s$) to accurately simulate their mechanical behavior during injuries.

The influence of strain rate on ACL and the patellar tendon (PT), which is usually used as a graft material for the ACL surgical reconstruction, was studied by Danto and Woo.⁽²⁸⁾ Tensile failure tests were performed on rabbit ACL-bone complexes at strain rates of 0.016%/s, 1.68%/s, and 381%/s and on PT-bone complexes at strain rates of 0.016%/s, 1.33%/s, and 135%/s. With few exceptions, failure occurred at the insertion sites of the ligaments to the bone. The tangent modulus of the ACLs was found to increase by 40% only when the strain rate increased by more than four decades. On the other hand, the tangent modulus was reported to increase by 94% for PTs over a range of four decades of strain rate. It was concluded that the PT is more sensitive to strain rate than the ACL.

Lydon et al. conducted tensile tests on the ACL-bone complex specimens using immature rabbits as animal models at 0.1 mm/s and 920 mm/s rates of elongation.⁽⁵⁰⁾ They demonstrated that the average linear stiffness, the ultimate load, ultimate deformation, and the energy at failure are affected by the elongation rate. In particular, the linear stiffness

and the ultimate load have been observed to increase with the elongation rate. Differently from other studies,^(24,28,49) the ultimate deformation was observed to decrease with increasing elongation rate. Furthermore, the mode of failure was confirmed to be rate dependent. Failure occurred by bony avulsions at the slower elongation rate and by fibrous avulsions at the higher elongation rate in agreement with previous studies.⁽⁴⁹⁾

The strain rate effects on human cruciate ligaments and PTs and on bovine ACL-bone complexes have been evaluated by Pioletti et al.^(25,26) By performing tensile tests at 0.3, 6, 9, and 12 mm/s strain rates on the human PTs and at 0.1, 1, 5, 10, 20, 30, 40%/s strain rates on bovine ACL, it was shown that the toe region of the stress-strain curves changes with the strain rate while the linear region of the curves remains unaffected. These results are in agreement with previous findings in which canine ACLs were tested under strain rates lower than 1%/s.⁽⁵¹⁾ They indicated that more fluid flows in the ligamentous tissue at the toe region of the stress-strain relationship, before the collagen fibers align in the direction of applied load.

Traumatic elongation rates, which correspond to 3660%/s and 14,000%/s strain rates, were used to determine the strain rate sensitivity of MCLs.⁽⁵²⁾ The results suggested that the strain rate does not affect significantly the load-elongation curve. However, the mechanical testing of the ligaments was performed without keeping the specimens in a saline bath. Thus, tissue dehydration may have occurred obfuscating the real mechanical properties of the ligaments.

The different findings in the above experimental studies are determined by various factors such as variations in species, age, strain measurements, and testing conditions. Moreover, it must be noted that comparisons among these studies are impossible since strain/elongation and stress/load rates are not carefully defined. Thus, suitable constitutive models are needed to provide an integrated understanding of the reported variations in strain rate effects for knee ligaments.

The short-time memory of ligaments have been described by various phenomenological models.^(25,28,53-56) The simplest equations used to capture the strain rate dependent behavior of soft biological tissues were formulated by combining spring and dashpot elements in series and in parallel.^(53,54) The validity of these equations is restricted to small deformations. Haut and Little proposed a constitutive model based on the quasi-linear viscoelastic theory advocated by Fung.⁽⁹⁾ Their model was shown to be able to reproduce the stress-strain curves of rat tail tendons only at low strain rates ranging from 0.06%/s to 0.75%/s. Danto and Woo adopted an empirical nonlinear elastic relationship to fit the stress-strain curve of ACLs and PTs at different strain rates.⁽²⁸⁾

The most attractive theoretical framework for the description of the short-time memory of soft tissues was proposed by Pioletti and colleagues.⁽²⁵⁾ They presented a three-dimensional constitutive law that modeled the strain rate sensitivity, nonlinearity, and incompressibility of ligaments and tendons. The constitutive equation was formulated by introducing an elastic potential and a viscous potential which are defined as functions of strain and strain invariants. It is valid for large deformations and it is thermodynamically admissible. It was tested by using uniaxial stress-strain data obtained from the human ACL, PCL and PT at different strain rates and by assuming the isotropy of these tissues. In a recent work,⁽⁵⁶⁾ Limbert and Middletown improved the constitutive model by assuming the ligaments to be transversely isotropic. Specific forms of the elastic and viscous potentials were derived and their material parameters were identified by using published uniaxial experimental data for human ACLs. Furthermore, the predictive capabilities of the model were investigated by considering various states of deformation.

Although the cited viscohyperelastic models^(25,56) faithfully reproduced the strain rate dependent properties of ligamentous tissues, they were unable to clarify the relation between the morphology of these tissues and their gross mechanical response. Thus, the first objective of the present study is to develop a constitutive model to accurately describe the ligament mechanical behavior based on the collagen fibrous structure.

By taking into account the orientation, the crimping, and the viscoelastic component of collagen fibers, the model simulates the strain rate effects on the mechanical response of the ligaments. Available experimental data for ACL from the literature^(26,28) are used to partially assess the model.

2.2 MODEL FORMULATION

An incompressible, three-dimensional constitutive law is proposed that is based on the collagenous fibrous structure of most ligaments. It is a modification of structural constitutive relations for soft tissues, originally proposed by Lanir,^(39,41) that incorporates strain rate effects. In the following formulation, the fibrous network is comprised of variously undulated fibers oriented in different directions. Collagen fibers are undulated in the slack configuration and unable to support load. They are gradually straightened under strain, at which point they manifest a viscoelastic behavior. Both the spatial arrangement and the waviness of the collagen fibers are defined stochastically.

2.2.1 Constitutive Equation

The existence of elastic and viscous potentials, $W_e(\mathbf{C})$ and $W_v(\mathbf{C}, \dot{\mathbf{C}})$, respectively, is assumed such that the first Piola-Kirchhoff stress tensor \mathbf{P} can be expressed as

$$\mathbf{P} = -p\mathbf{F}^{-\top} + 2\mathbf{F} \cdot \left(\frac{\partial W_e(\mathbf{C})}{\partial \mathbf{C}} + \frac{\partial W_v(\mathbf{C}, \dot{\mathbf{C}})}{\partial \dot{\mathbf{C}}} \right), \quad (2.1)$$

where p is an indeterminate pressure enforcing the incompressibility assumption, \mathbf{F} is the deformation gradient tensor, \mathbf{F}^\top and $\mathbf{F}^{-\top}$ are its transpose and inverse transpose, respectively, $\mathbf{C} \equiv \mathbf{F}^\top \cdot \mathbf{F}$ is the right Cauchy-Green deformation tensor, and $\dot{\mathbf{C}}$ is its material time derivative.^(25,57) A “dot product” notation is used, wherein a vector \mathbf{u} is mapped by a second-order tensor \mathbf{A} into the vector $\mathbf{A} \cdot \mathbf{u}$ and the composition of two second-order tensors

\mathbf{A} and \mathbf{B} is another second-order tensor denoted by $\mathbf{A} \cdot \mathbf{B}$, so that $(\mathbf{A} \cdot \mathbf{B}) \cdot \mathbf{u} = \mathbf{A} \cdot (\mathbf{B} \cdot \mathbf{u})$ for an arbitrary vector \mathbf{u} . The last expression thus admits the unambiguous representation $\mathbf{A} \cdot \mathbf{B} \cdot \mathbf{u}$. The tensor product of two vectors \mathbf{u} and \mathbf{v} is a second-order tensor denoted by \mathbf{uv} and defined such that $\mathbf{uv} \cdot \mathbf{a} = (\mathbf{uv}) \cdot \mathbf{a} = \mathbf{u}(\mathbf{v} \cdot \mathbf{a})$ for an arbitrary vector \mathbf{a} .

In the absence of the viscous potential, (2.1) yields the usual dissipation-free, incompressible hyperelastic response. Thus, the assumed viscous potential $W_v(\mathbf{C}, \dot{\mathbf{C}})$ accounts for dissipation.⁽²⁵⁾ Sufficient conditions for satisfaction of the Clausius-Duhem inequality are that the viscous potential be continuous, non-negative, and convex and that $W_v(\mathbf{C}, \mathbf{0}) = 0$.

Let $R(\hat{\mathbf{M}})$ be the probability density for collagen fibers whose mean axes in the reference configuration are parallel to the unit vector $\hat{\mathbf{M}}$. Both the elastic and the viscous potentials are assumed to be determined solely by the collagen fibers' extension—shear and bending energies are not taken into account. Accordingly, it is assumed that the elastic and viscous potentials can be represented as

$$W_e(\mathbf{C}) = \int_{\Sigma} R(\hat{\mathbf{M}}) w_e(\Lambda(\mathbf{C}, \hat{\mathbf{M}})) d\Sigma, \quad (2.2)$$

$$W_v(\mathbf{C}, \dot{\mathbf{C}}) = \int_{\Sigma} R(\hat{\mathbf{M}}) w_v(\Lambda(\mathbf{C}, \hat{\mathbf{M}}), \dot{\Lambda}(\mathbf{C}, \dot{\mathbf{C}}, \hat{\mathbf{M}})) d\Sigma, \quad (2.3)$$

where Σ is the set of all material directions and $w_e(\Lambda)$ and $w_v(\Lambda, \dot{\Lambda})$ are the collagen fiber elastic and viscous potentials corresponding to axial fiber stretch Λ and stretch rate $\dot{\Lambda}$, given by

$$\Lambda(\mathbf{C}, \hat{\mathbf{M}}) = \sqrt{\hat{\mathbf{M}} \cdot \mathbf{C} \cdot \hat{\mathbf{M}}}, \quad \dot{\Lambda}(\mathbf{C}, \dot{\mathbf{C}}, \hat{\mathbf{M}}) = \frac{1}{2} \frac{\hat{\mathbf{M}} \cdot \dot{\mathbf{C}} \cdot \hat{\mathbf{M}}}{\sqrt{\hat{\mathbf{M}} \cdot \mathbf{C} \cdot \hat{\mathbf{M}}}}. \quad (2.4)$$

Introducing the fiber elastic stress $\sigma_e(\Lambda)$ and the fiber viscous stress $\sigma_v(\Lambda, \dot{\Lambda})$ as follows

$$\sigma_e(\Lambda) \equiv \frac{dw_e(\Lambda)}{d\Lambda}, \quad \sigma_v(\Lambda, \dot{\Lambda}) \equiv \frac{\partial w_v(\Lambda, \dot{\Lambda})}{\partial \dot{\Lambda}}, \quad (2.5)$$

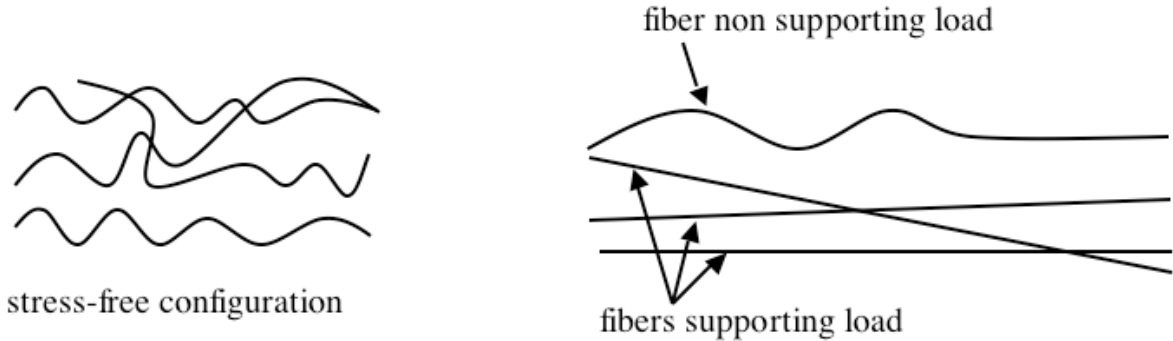


Figure 2.1. Assumptions in the recruitment model.

the constitutive equation (2.1) then assumes the form

$$\mathbf{P} = -p\mathbf{F}^{-\top} + \mathbf{F} \cdot \int_{\Sigma} R(\hat{\mathbf{M}}) \frac{\hat{\mathbf{M}}\hat{\mathbf{M}}}{\Lambda(\mathbf{C}, \hat{\mathbf{M}})} [\sigma_e(\Lambda(\mathbf{C}, \hat{\mathbf{M}})) + \sigma_v(\Lambda(\mathbf{C}, \hat{\mathbf{M}}), \dot{\Lambda}(\mathbf{C}, \dot{\mathbf{C}}, \hat{\mathbf{M}}))] d\Sigma. \quad (2.6)$$

Once the collagen fiber orientation distribution $R(\hat{\mathbf{M}})$ and axial constitutive relations $\sigma_e(\Lambda)$ and $\sigma_v(\Lambda, \dot{\Lambda})$ have been specified, relation (2.6) can be employed to predict the ligament's strain rate dependent behavior. In the next section, the axial constitutive equations will be specified by considering the fibers' initial crimping and straightening under deformation.

2.2.2 Recruitment Model

The fiber recruitment model, which is characterized statistically by a probability density function for the stretch necessary to straighten a crimped fiber, has been employed by a number of researchers in biomechanics.^(37, 39–41, 43, 44, 46, 58, 59) The novelty of the proposed model is in the introduction of collagen fibers' viscous effects to describe the ligament's strain rate effect.

Collagen fibers are undulated, or crimped, in the stress-free configuration. They are assumed to support load only after becoming taut—the load necessary to straighten the

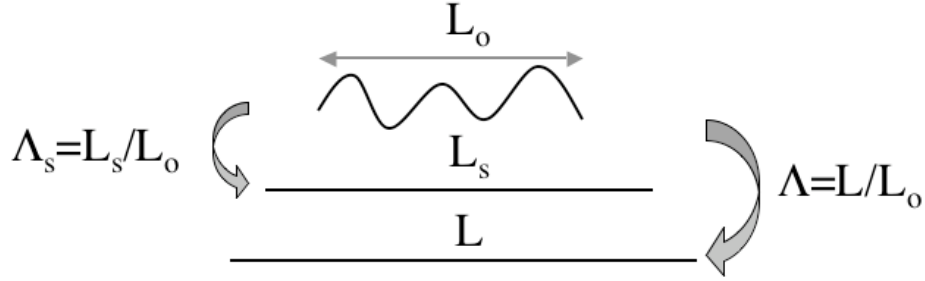


Figure 2.2. Λ : axial fiber stretch, Λ_s : straightening stretch.

fibers is assumed to be negligible in comparison. Thus, the fiber elastic and viscous stresses are given by

$$\sigma_e(\Lambda) = \int_1^\Lambda g(\Lambda_s) \hat{\sigma}_e\left(\frac{\Lambda}{\Lambda_s}\right) d\Lambda_s, \quad (2.7)$$

$$\sigma_v(\Lambda, \dot{\Lambda}) = \int_1^\Lambda g(\Lambda_s) \hat{\sigma}_v\left(\frac{\Lambda}{\Lambda_s}, \frac{\dot{\Lambda}}{\Lambda_s}\right) d\Lambda_s, \quad (2.8)$$

where $g(\Lambda_s)$ is the probability density for fibers which become taut at a stretch Λ_s and Λ/Λ_s is the stretch with respect to the fiber's taut configuration (See Figure 2.2). The probability density must satisfy the normality condition $\int_1^\infty g(\Lambda) d\Lambda = 1$. The values of $\hat{\sigma}_e(\Lambda_t)$ and $\hat{\sigma}_v(\Lambda_t, \dot{\Lambda}_t)$ represent the elastic and viscous stresses for a taut fiber stretched an amount $\Lambda_t = \Lambda/\Lambda_s$ and with a stretch rate of $\dot{\Lambda}_t = \dot{\Lambda}/\Lambda_s$. They are subject to the constraints $\hat{\sigma}_e(1) = 0$ and $\hat{\sigma}_v(\Lambda, 0) = 0$.

2.2.3 Fiber Elastic and Viscous Stresses

The structural model presented above correlates the gross mechanical response of the ACL to the collagen fibers' mechanical response. Each collagen fiber is assumed to have a Kelvin-Voigt-type viscoelastic constitutive behavior based on studies by Sasaki and Odajima.⁽⁶⁰⁾

By using an x-ray diffraction method, these authors found that the stress-strain relationship for the collagen molecule in tendons is almost linear. Moreover, after comparing their findings with previous studies,⁽⁶¹⁾ they speculated that the mechanical properties of the tropocollagen are strain rate dependent. The three α -chains, which form the helix structure of the collagen molecule, are stabilized by hydrogen bonds (See Figure 1.3). The hydrogen bonds are bind to water molecules and, when the molecule is hydrated, these water molecules exchange with other water molecules. The disruption and the reformation of these bonds produces energy dissipation. Therefore, the strain rate dependent behavior of the tropocollagen is believed to be determined by the network of hydrogen bonds.⁽⁶⁰⁾

There is often some ambiguity in reported experimental results regarding the precise definition of the measured strains. Assuming that the strain measured is the logarithmic strain, $\varepsilon \equiv \ln \Lambda$, the elastic and viscous stresses for a taut fiber are taken as

$$\hat{\sigma}_e(\Lambda_t) = K \ln \Lambda_t, \quad \hat{\sigma}_v(\Lambda_t, \dot{\Lambda}_t) = \eta (\ln \Lambda_t) \dot{\Lambda}_t = \frac{\eta \dot{\Lambda}_t}{\Lambda_t}, \quad (2.9)$$

where K is the *elastic stiffness* and η is the *coefficient of viscosity*. Alternatively, one could assume that the reported strain is the engineering strain, $\varepsilon_0 \equiv \Lambda - 1$, and accordingly that

$$\hat{\sigma}_e(\Lambda_t) = K_0(\Lambda_t - 1), \quad \hat{\sigma}_v(\Lambda_t, \dot{\Lambda}_t) = \eta_0 \dot{\Lambda}_t, \quad (2.10)$$

where K_0 and η_0 are constants.

The maximum strain in the data used below, from Danto and Woo⁽²⁸⁾ and Pioletti et al.,⁽²⁶⁾ is less than 10%. At this strain, the relative difference between the two interpretations of the reported strain is $\sim 0.5\%$. That is, if $\varepsilon = 0.1$ then $\varepsilon_0 = 0.1052$ and if $\varepsilon_0 = 0.1$ then $\varepsilon = 0.0953$. While this difference is significant, it likely falls within the margin of experimental error for the data considered here. Nonetheless, it would be beneficial if experimentally determined strains (and stresses) are more clearly defined when reported. The logarithmic strain is assumed here.

2.3 MODEL IMPLEMENTATION

In order to evaluate the capability of the proposed model, published tensile test data obtained for the ACL at various strain rates will be used. To this end, an homogenous axisymmetric deformation is considered. Moreover, the ACL is assumed to have a perfectly collagenous parallel-fibered structure and the recruitment process is governed by a modified Weibull distribution.

2.3.1 Isochoric, Axisymmetric Deformation

In order to compare the model with the uniaxial loading experiments reported by Danto and Woo⁽²⁸⁾ and Pioletti et al.,⁽²⁶⁾ the isochoric deformation is assumed to be axisymmetric with a deformation gradient of the form

$$\mathbf{F} = \lambda^{-\frac{1}{2}} \mathbf{e}_r \mathbf{E}_R + \lambda^{-\frac{1}{2}} \mathbf{e}_\theta \mathbf{E}_\Theta + \lambda \mathbf{e}_z \mathbf{E}_Z, \quad (2.11)$$

where the axial stretch $\lambda(t)$ is a function of time t that satisfies $\lambda(0) = 1$.⁽⁶²⁾ The orthonormal bases $\{\mathbf{E}_R, \mathbf{E}_\Theta, \mathbf{E}_Z\}$ and $\{\mathbf{e}_r, \mathbf{e}_\theta, \mathbf{e}_z\}$ are defined such that \mathbf{E}_Z and \mathbf{e}_z are unit vectors parallel to the direction of loading in the reference and current configurations, respectively (See Figure 2.3). The corresponding right Cauchy-Green deformation tensor is thus given by

$$\mathbf{C} = \lambda^{-1} \mathbf{E}_R \mathbf{E}_R + \lambda^{-1} \mathbf{E}_\Theta \mathbf{E}_\Theta + \lambda^2 \mathbf{E}_Z \mathbf{E}_Z. \quad (2.12)$$

2.3.2 Collagen Fiber Orientation and Crimp

In the reference configuration, the mean axial directions of the collagen fibers are assumed to be aligned along the direction of loading, \mathbf{E}_Z , so that the probability density for fiber orientation is $R(\hat{\mathbf{M}}) = \delta(\hat{\mathbf{M}} - \mathbf{E}_Z)$, where δ is the Dirac delta function (See Figure 2.3).

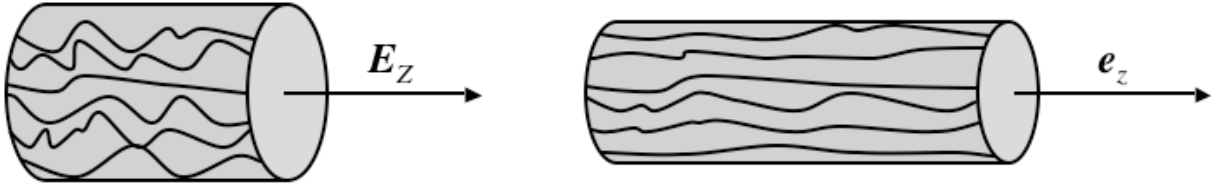


Figure 2.3. Reference configuration (right) and current configuration (left).

It then follows from (2.4), (2.6), (2.11), and (2.12) that the non-zero components of the first Piola-Kirchhoff stress are given by

$$P_{rR} = P_{\theta\Theta} = -p\lambda^{\frac{1}{2}}, \quad P_{zZ} = -p\lambda^{-1} + \sigma_e(\lambda) + \sigma_v(\lambda, \dot{\lambda}). \quad (2.13)$$

The traction-free boundary condition on the lateral surface of the test specimen thus implies that the indeterminate pressure term must vanish, $p = 0$. The recruitment model, (2.7) and (2.8), and the assumed form of the fiber response (2.9) then give

$$P_{zZ} = \int_1^\lambda g(\lambda_s) \left[K \ln \frac{\lambda}{\lambda_s} + \eta \left(\ln \frac{\lambda}{\lambda_s} \right) \right] d\lambda_s \quad (2.14)$$

as the only non-zero component of stress.

The crimp probability density is taken to be a modified Weibull function of the following form:

$$g(\lambda) = \alpha\beta^{-\alpha}\lambda^{-1}(\ln \lambda)^{\alpha-1}e^{-(\ln \lambda/\beta)^\alpha}, \quad (2.15)$$

where $\alpha > 0$ is the shape parameter and $\beta > 0$ is the scale parameter. This probability density function is one-sided, with $g(1) = g(\infty) = 0$ and satisfies the normality condition $\int_1^\infty g(\lambda) d\lambda = 1$. The corresponding cumulative probability function is

$$G(\lambda) = \int_1^\lambda g(\lambda_s) d\lambda_s = 1 - e^{-(\ln \lambda/\beta)^\alpha}. \quad (2.16)$$

The change of variable $\lambda_s = e^{\varepsilon_s}$ in (2.14) and (2.15) then yields

$$P_{zZ} = \int_0^\varepsilon \alpha \beta^{-\alpha} \varepsilon_s^{\alpha-1} e^{-(\varepsilon_s/\beta)^\alpha} [K(\varepsilon - \varepsilon_s) + \eta \dot{\varepsilon}] d\varepsilon_s . \quad (2.17)$$

This relation gives the nominal axial stress P_{zZ} as a function of the logarithmic axial strain and strain rate, ε and $\dot{\varepsilon}$, and the four material parameters K , η , α , and β , which are estimated by curve fitting data from tensile tests.

2.4 RESULTS

Because of the complexities involved in conducting high strain rate experiments on collagenous tissue, there are few studies on the stress-strain relationship at such strain rates in the biomechanical literature. Published experimental stress-strain data from rabbit and bovine ACL-bone complexes^(26,28) have been used to assess the proposed model. In these studies the effects of strain rate on the mechanical response of the ligamentous tissue have been investigated. Several factors such as species, age, and, most importantly, testing methodologies, have contributed to differences in the experimental findings on the ACL-bone complex rheological behavior.

Danto and Woo⁽²⁸⁾ have tested the medial portion of rabbit ACL-bone complex by performing tensile tests at three strain rates: 0.016%/s, 1.68%/s and 381%/s. In their study, they have not observed a significant difference in the ACL mechanical properties between the strain rates of 0.016%/s and 1.68%/s. Hence, in order to determine the parameter values in the material law, (2.17) has been fitted using the stress-strain data at 1.68%/s and 381%/s strain rates. By implementing the Levenberg-Marquardt nonlinear least-squares algorithm and by constraining the parameters to be positive, the best-fit parameters have been found to be $\alpha = 1.5$, $\beta = 0.038$, $K = 840$ MPa, and $\eta = 5.1$ MPa/s. Figure 2.4 illustrates the good-

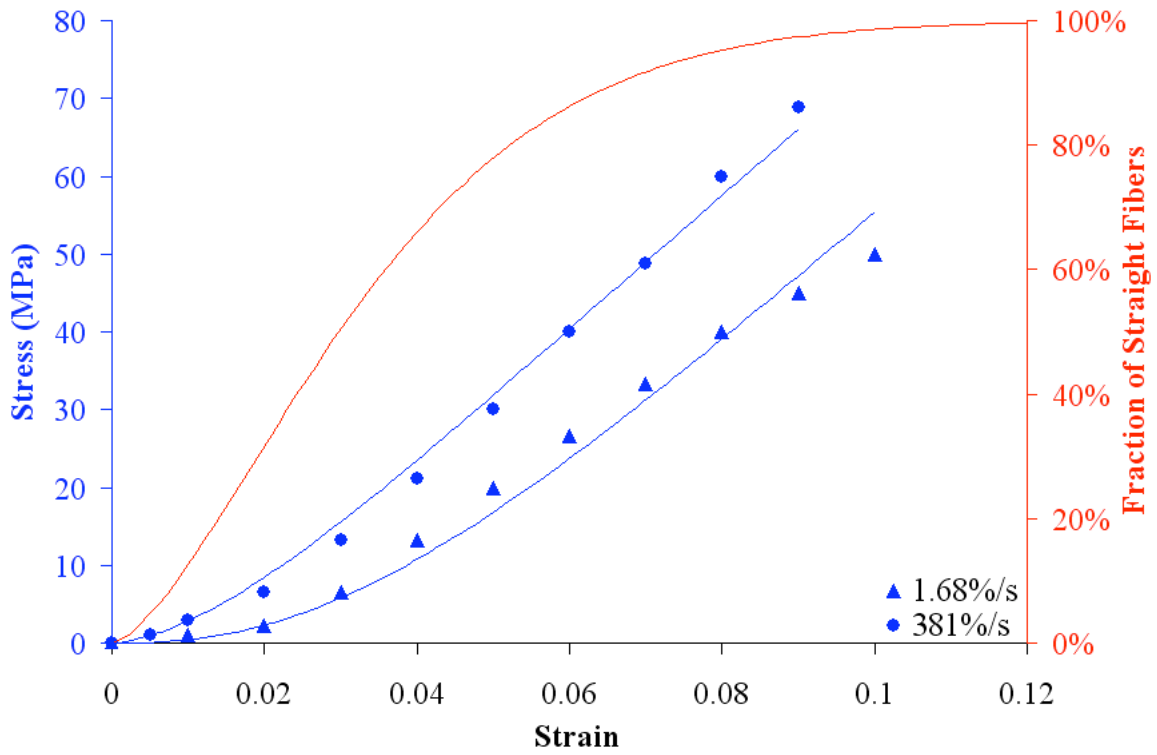


Figure 2.4. Stress-strain experimental data from Danto and Woo⁽²⁸⁾ at 1.68%/s and 381%/s strain rates with model (—) and fraction of straight fibers (—) evaluated at best fitting parameters.

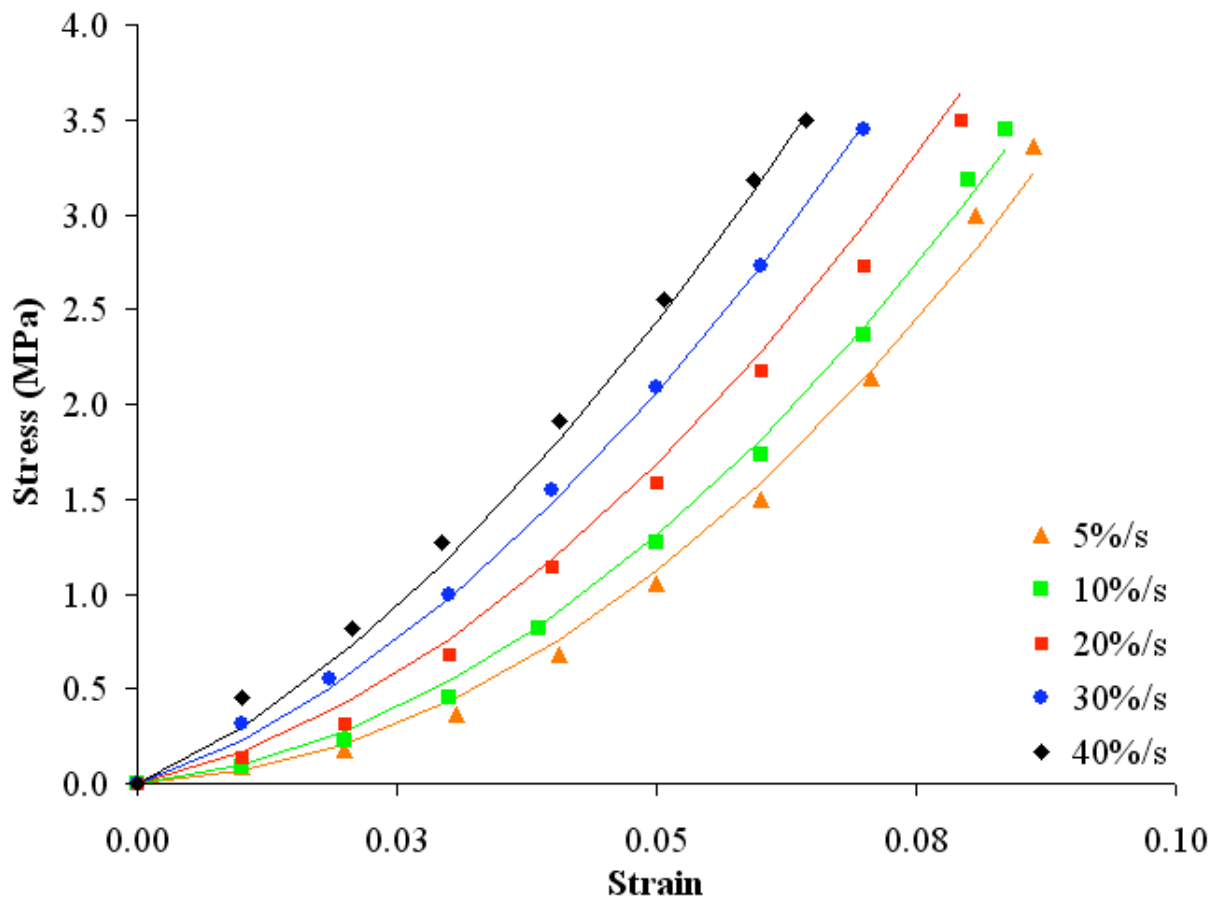


Figure 2.5. Experimental data from Pioletti and co-authors⁽²⁶⁾ at 5%/s, 10%/s, 20%/s, 30%/s, and 40%/s strain rates (various symbols) and theoretical stress-strain curves (continuous line).

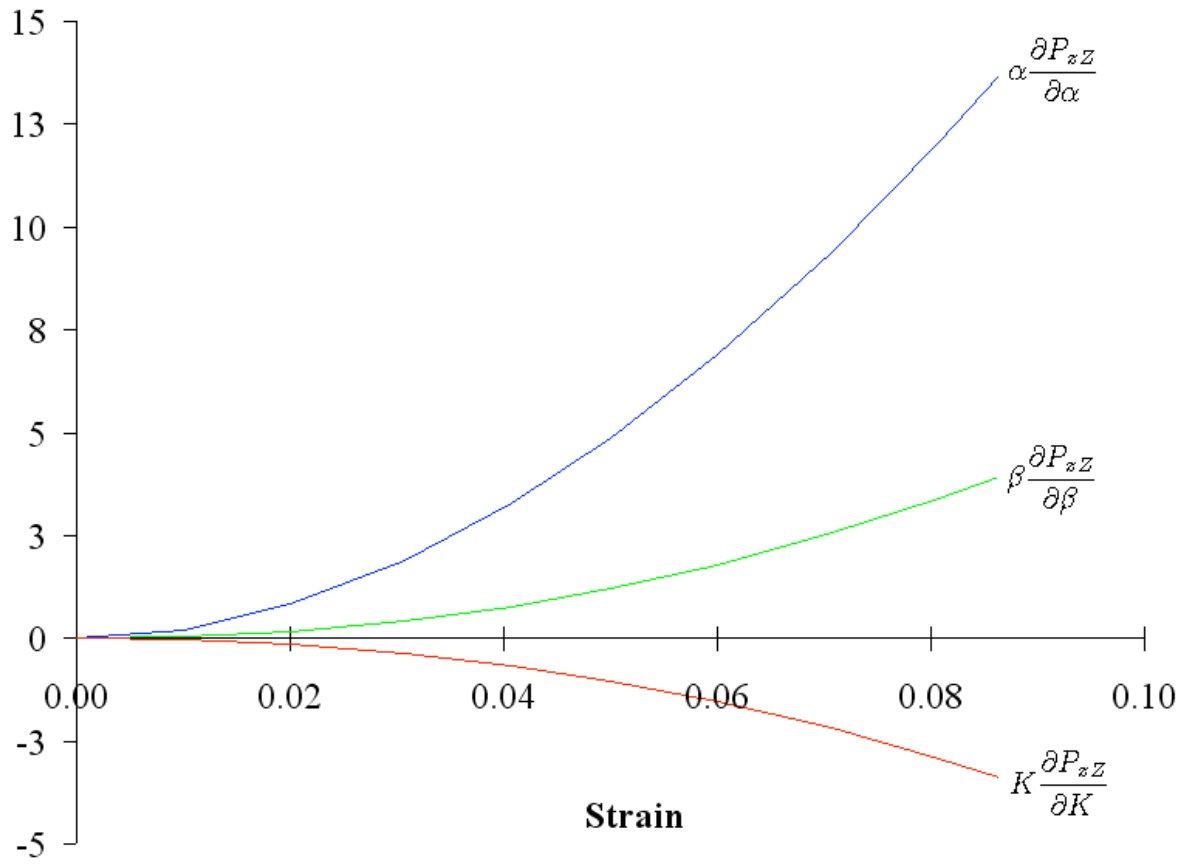


Figure 2.6. Linear dependence of the sensitivity coefficients.

ness of the fit to the experimental data ($R^2 = 0.97$) together with the fraction of straight fibers as defined by the cumulative probability $\tilde{G}(\varepsilon) \equiv G(e^\varepsilon) = 1 - e^{-(\varepsilon/\beta)^\alpha}$. The model predicts a stiffening of the toe region with increasing strain rate. The cumulative probability shows the fraction of the fibers recruited for various values of strain. For instance, it can be observed that 90% of collagen fibers are recruited at 6.6% strain.

Pioletti et al.⁽²⁶⁾ have conducted tensile tests at several strain rates (0.1%/s, 1%/s, 5%/s, 10%/s, 20%/s, 30%/s, 40%/s) on bovine ACL-bone complexes. They have demonstrated that the strain rate affects mainly the toe region of the stress-strain relationship while leaving almost unaffected the tangent modulus of the linear region. An attempt to fit the data of Pioletti et al. with the constitutive equation (2.17) has been made. Equation (2.17) fits the experimental stress-strain curves very well with $R^2 > 0.99$ (See Figure 2.5), although a unique set of fitting parameters could not be determined because the identifiability criterion is not satisfied.^(63,64) According to this criterion, the sensitivity coefficients of the model, $K\partial P_{zz}/\partial K$, $\eta\partial P_{zz}/\partial\eta$, $\alpha\partial P_{zz}/\partial\alpha$, and $\beta\partial P_{zz}/\partial\beta$, must be linearly independent in the neighborhood of the minimum sum of squares function, over the range of measurements. To illustrate the criterion, the sensitivity coefficients of the model, which have been obtained by setting $\eta = 0$ and by fitting the stress-strain data at 5%/s strain rate, are depicted in Figure 2.6. The fitting parameters cannot be uniquely determined since $K\partial P_{zz}/\partial K + \beta\partial P_{zz}/\partial\beta$ approaches to zero and, hence, $K\partial P_{zz}/\partial K$ and $\beta\partial P_{zz}/\partial\beta$ are approximately linearly dependent.

2.5 DISCUSSION

A constitutive law for knee ligaments is formulated by modifying the structural theory proposed by Lanir^(39,41) to include a description of strain rate dependent effects. The nonlinear material response, the anisotropy, the finite deformation, and the incompressibility of ligamentous tissue are taken into account. The model has the merit of being structurally based,

with the material parameters directly associated with the tissue’s main constituents. It has been shown to be capable of characterizing the typical mechanical properties of the ACL with only four parameters. The initially wavy collagen fibers in the ligament become straight when subjected to a load and the tissue’s overall stress-strain relationship stiffens exponentially. Consequently, the taut collagen fibers sustain the load and, hence, they are responsible for the high modulus response. The novelty of the model is in capturing, in the toe region, an increase in the mechanical properties of the ligament with strain rate. No differences in the slopes of the linear region of the stress-strain curves are predicted. These results are in accordance with the observations made by Pioletti et al. for bovine ACL.⁽²⁶⁾

A good fit of the model with the experimental results by Danto and Woo⁽²⁸⁾ was attained. The estimated parameters α and β defined a distribution which describes the sequential straightening of collagen fibers as the ACL-bone complex elongates. The one-sided probability density function was selected in order to exclude the unrealistic possibility that collagen fibers straighten out in compression. In particular, the results indicated that the transition from the toe region to the linear region of the stress-strain curve occurs with a smaller percentage of fibers recruited when the strain rate is faster. It is worth noting that recent studies have established that the Weibull probability function with a nonzero location parameter can be employed to determine the reference length of the ligament.⁽⁶⁵⁾ Therefore, the assumption of an initial slack configuration could be removed by introducing an additional parameter into the model.

The collagen fiber elastic modulus was found to have a value, $K = 840$ MPa, which is comparable with the 0.4 GPa and 1 GPa values reported in the biomechanical literature.^(9, 60, 66) It should be noted that the stiffness K in the current model is actually underestimated. This is because, in the model formulations, collagen fibers are assumed to occupy the whole cross sectional area of the ACL while the other ligamentous constituents have been neglected. By the same argument, the value for η is also underestimated.

When considering the experimental data from Pioletti et al.,⁽²⁶⁾ it was not possible to identify a unique set of material constants by implementing the Levenberg-Marquardt non-linear data fitting procedure and by constraining the parameters to be positive. The identifiability criterion utilizing sensitivity coefficients was invoked.^(63,64) Indeed, the sensitivity coefficients were found to be linearly dependent. This emphasizes the need for experiments designed to accurately evaluate the parameters in the constitutive model. It is speculated that the non-uniqueness is caused by the absence of a prolonged linear region in the experimental stress-strain curves.

The proposed constitutive relation has been tested under the assumption that all collagen fibers are perfectly parallel in the ligament. This assumption can be removed when quantification of the initial fiber orientation is obtainable. Sacks^(46,48) showed that information on collagen fiber organization in planar tissues can be gained by using a small angle light scattering technique and, subsequently, incorporated into structural models. Similar techniques could help to determine the collagen fiber orientation in the ligament.⁽⁶⁷⁾ Moreover, because histological studies clarifying the role of each component in the ligaments are still not available, the matrix and elastin fiber contributions together with the interactions among the various constituents are not included in the proposed model.

The collagen fiber behavior was modeled using a Kelvin-Voigt element, which is characterized by a linear dependence on the strain rate. It must be noted that the strain rate dependent effects are considered to be due solely to the collagen fibers. This assumption is supported by Sasaki and Odajima.⁽⁶⁰⁾ In their study, it was speculated that the modulus of the collagen molecule increases with strain rate. Nevertheless, it may be possible that strain rate effects are due to a fluid-like matrix or/and intermolecular cross-linking.

Experimental multiaxial data need to be used to accurately test the model's capability to predict the mechanical response of the ACL under various loading conditions. Tensile tests are not sufficient alone to fully characterize the mechanics of the tissue. Strain measurements at high strain rates over the entire ligament are required to establish the ACL biomechanics.

The present study is unique in that it is the first time that a structural constitutive model has been used to reproduce the strain rate sensitivity of ACL revealed in experimental investigations. Lanir⁽⁴¹⁾ developed a very *general* viscoelastic constitutive theory for the lung tissue which was not validate by using experimental data. In the present study, a *specific* viscoelastic constitutive equation is formulated and successfully tested with experimental data for the ACL. It is believed that the formulation of a reliable constitutive equation in conjunction with appropriate experimental works can lead to a better understanding of the mechanisms of ACL injury.

3.0 A STRUCTURAL MODEL FOR THE FAILURE BEHAVIOR

3.1 FAILURE BEHAVIOR OF KNEE LIGAMENTS

The most severe injuries of the ligaments are partial and complete tears commonly known as second-degree and third-degree sprains, respectively. Tears of the knee ligaments can lead to chronic instabilities of the joint and can often prevent the return of athletic patients to sport activities. Understanding the mechanism of tearing in ligamentous materials is thus important for the prevention, the diagnosis and the treatment of these injuries. Toward this end, experimental investigations complemented with reliable constitutive descriptions are needed to study the disruption of the ligamentous fibers associated with the injuries.

Several experimental studies have been carried out to determine the mechanical properties of the knee ligaments. The progress in experimental technologies has significantly contributed to characterize the mechanics of these ligaments. Nevertheless, difficulties persist in accurately establishing the material properties of the ligamentous tissue and in exploring the role of the tissue's components during injuries.

As noted earlier, most of the experimentalists have measured the tensile properties of ligaments (Section 1.3). Tensile tests are usually performed on femur-ligament-tibia complexes due to the problems in clamping the ligamentous substance and due to the necessity of simulating in vivo loading conditions. During these tests, the ligament can thus fail in the mid-substance, at the insertion sites, or by bony avulsion. Failure at the insertion sites consists of the net separation of the ligamentous substance from the bone. Bony avulsion is a failure of the bone-ligament complex involving the disruption of the osseous substance. However, the material properties of the ligament—tangent modulus, ultimate strain, and

tensile strength—are computed only when failure occurs in the ligamentous substance or at the insertion sites.⁽⁵⁾ It is then clear that experiments designed to study the failure of the ligamentous material can be time-consuming and require costly animal trials.

The strain field is reported to be inhomogeneous over the entire surface of the knee ligaments.^(68,69) Thus, in order to account for the material inhomogeneities, strain is often measured by video-recording the displacement of markers that are glued on the surface of the ligament. When the ligament is tearing, the markers come out of the surface region of the ligament, whose strain is being recorded, and, hence, analyzing the mechanical properties associated with tears is impracticable.

Because of the shortcomings in the experimental methods, the process of failure in ligaments remains poorly understood. It is believed that the development of suitable structural constitutive relationships may play a significant role in comprehending the mechanisms of the ligamentous injuries. The structural framework can help delineating the relationship between the biological architecture and the mechanical failure behavior of ligaments.

Structural modeling of the collagenous tissue failure behavior has already received the attention of several investigators. Kwan and Woo⁽⁷⁰⁾ developed a one-dimensional microstructural model for parallel-fibered collagenous tissues in which collagen fibrils were assumed to be responsible for the gross tissue nonlinear response. In their model, the tissue was considered to be composed of groups of fibrils with different initial lengths, uncrimping strains, and failure strains. Collagen fibril stress-strain relationship was assumed to be bilinear. The model fitted the rabbit ACL and canine MCL experimental data but eleven parameters were needed.

The most complete theoretical description of failure for ligaments and tendons has been presented by Hurschler et al.⁽⁵⁹⁾ The constitutive law was formulated by modeling the collagen fiber, the matrix and the fibril structures. The tissue stress-stretch relationship was defined by considering the sequential uncrimping and stretching of collagen fibers. The fiber recruitment process was defined by a one-sided distribution. Moreover, the constitutive law

for individual fiber was determined by the fibril kinematics and spatial orientation. The matrix was assumed to contribute to the gross mechanical behavior through a hydrostatic pressure term. Stretch-based failure criteria were introduced in the model at fibril level for disorganized tissue and at the fiber level for parallel-fibered tissues. In both cases, the failure stretch was assumed to be equal for all fibrils or for all the straight fibers. The constitutive relation was simplified in order to curve fit experimental data of healing rabbit and rat MCLs. However, the values of the best fitting material parameters were not reported by the authors and, perhaps, could not be uniquely determined.

In a follow-up study, Liao and Belkoff⁽⁶⁶⁾ presented a failure model for the tensile properties of ligaments that incorporates the collagen fiber gradual recruitment and stretching. The fiber recruitment was described by a two-sided distribution and, therefore, some fibers could unrealistically become straight at a negative stretch. Each collagen fiber was assumed to be linear elastic and to fail at the same stretch in the taut configuration. This model has the merit of containing only four structural parameters. Although the model was found to describe well the abrupt failure behavior, it could not reproduce the gradual failure behavior observed in experimental studies on rabbit MCLs.

Wren and Carter⁽⁷¹⁾ proposed a structural law for the tensile constitutive pre-failure and failure behavior of soft skeletal connective tissues. The mathematical model accounts not only for the collagen fiber uncrimping, stretching, breakage, orientation and volume fraction but also for matrix constitutive behavior and its resistance to fiber reorientation. Experimental data from tendon, meniscus and articular cartilage were used to validate the model. The values of the structural parameters, which appear in the model, were extrapolated from various experimental studies.

The aforementioned constitutive models were able to illustrate the *abrupt* failure behavior of collagenous tissues. In this chapter, a novel structural constitutive model is formulated to describe the *gradual* tensile failure behavior of ligaments under the assumption that, after losing their waviness, fibers fail at different stretches. The model is validated by using

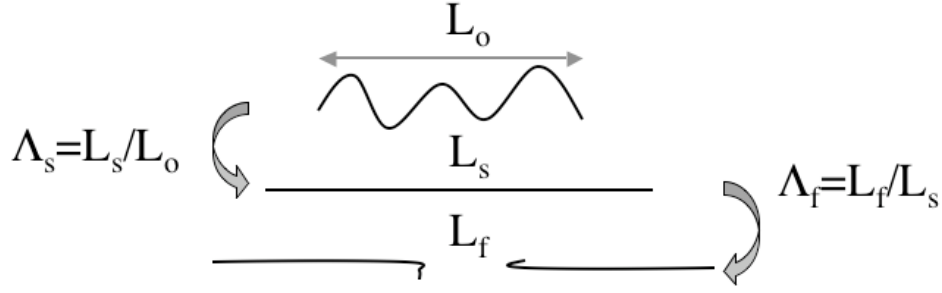


Figure 3.1. Λ_s : straightening fiber stretch, Λ_f : failure fiber stretch.

published stress-strain data for the MCL. Moreover, it is compared over a model which is based on the common assumption that the straight fibers in the tissue fail at an identical stretch. Although a three-dimensional model is proposed, it is not validated due to the lack of multi-axial histomechanical data for ligaments.

3.2 MODEL FORMULATION

A one-dimensional stochastic model is first presented to describe the tensile pre-failure and failure behaviors of ligaments. The ligament is idealized as composed of collagen fibers that are aligned along its direction of physiological loading. The fibers are assumed to be linear elastic and to possess the same stiffness. They contribute to the ligament's mechanical response after becoming taut and before breaking. The fiber bending and compressive stiffnesses are ignored as well as fiber-fiber and matrix-fiber interactions. Moreover, viscous effects are not taken into account. The failure criterion is stretch based but, differently from previous studies,^(59,66,71) the fibers in the tissue are postulated to break at different stretches. Both the fiber straightening and fiber breakage are statistically defined by Weibull cumulative distributions. Subsequently, a general three-dimensional material law is proposed based on Lanir's pioneering work in soft tissue structural constitutive modeling.^(39,41)

3.2.1 Recruitment and Failure Model

The mechanical response of the ligament is determined by the collagen component. Elastin fibers are not assumed to contribute to the mechanical behavior since their amount is not significant in these ligaments. (See Section 1.2). Thus, the ligament is assumed to be made up of N parallel collagen fibers, where N is an integer. In the reference configuration, the N collagen fibers are aligned along the main physiological loading direction of the ligament.

The generic collagen fiber i is characterized by a straightening stretch, $\Lambda_s^{(i)}$, and a failure stretch, $\Lambda_f^{(i)}$, where $i = 1 \dots N$ (See Figure 3.1). The straightening stretches and the failure stretches for the N fibers are randomly distributed according to Weibull cumulative distributions. Hence, they are given by

$$\Lambda_s^{(i)} = 1 + \beta_s [\ln(1 - G_s^{(i)})]^{-\frac{1}{\alpha_s}}, \quad \Lambda_f^{(i)} = 1 + \beta_f [\ln(1 - G_f^{(i)})]^{-\frac{1}{\alpha_f}}, \quad (3.1)$$

where $\alpha_s > 0$ and $\beta_s > 0$ are the shape and the scale parameters of the Weibull distribution describing fiber straightening and $\alpha_f > 0$ and $\beta_f > 0$ are the shape and the scale parameters of the Weibull distribution governing fiber failure. $G_s^{(i)}$ and $G_f^{(i)}$ are random numbers with $0 < G_s^{(i)} < 1$ and $0 < G_f^{(i)} < 1$.

The fibers are assumed to contribute to the overall tissue's stress only after losing their undulation and before failing (See Figure 3.2). Moreover, they are modeled as linear elastic material. Therefore, the stress-stretch relation for the generic fiber i is defined as follows

$$\sigma^{(i)} = \begin{cases} 0 & \frac{\Lambda}{\Lambda_s^{(i)}} \leq 1 ; \\ K \left(\frac{\Lambda}{\Lambda_s^{(i)}} - 1 \right) & 1 < \frac{\Lambda}{\Lambda_s^{(i)}} < \Lambda_f^{(i)} ; \\ 0 & \frac{\Lambda}{\Lambda_s^{(i)}} \geq \Lambda_f^{(i)} , \end{cases} \quad (3.2)$$

where K is the fiber stiffness, Λ is the overall tissue's stretch, and $\Lambda/\Lambda_s^{(i)}$ is the fiber stretch relative to the taut configuration.

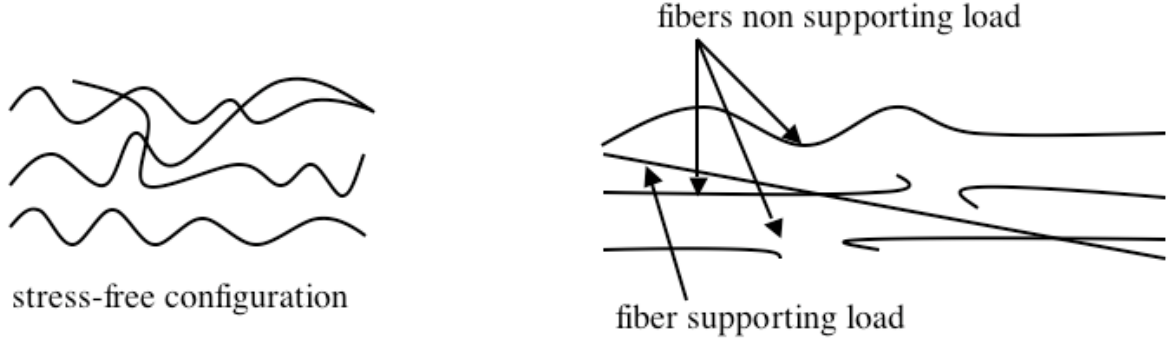


Figure 3.2. Assumption of the recruitment model with failure.

The overall tissue's stress, σ is defined as the average of the stresses of the N fibers. Thus, it is given by

$$\sigma(\Lambda) = \frac{1}{N} \sum_{i=1}^N \sigma^{(i)}. \quad (3.3)$$

Finally, a set of five material parameters, $\{K, \alpha_s, \beta_s, \alpha_f, \beta_f\}$, needs to be determined by curve-fitting experimental data to replicate the uniaxial stress-stretch relationship of ligaments.

3.2.2 Model Generalization

The one-dimensional model proposed in Section (3.2.1) can be generalized in order to describe the three-dimensional mechanical behavior of ligaments. The first Piola-Kirchhoff stress tensor \mathbf{P} can be expressed as⁽⁶⁾

$$\mathbf{P} = -p\mathbf{F}^{-\top} + 2\mathbf{F} \cdot \frac{\partial W(\mathbf{C})}{\partial \mathbf{C}}, \quad (3.4)$$

where ‘ \cdot ’ denotes the dot product, p is an indeterminate pressure enforcing the incompressibility assumption, \mathbf{F} is the deformation gradient tensor, \mathbf{F}^\top and $\mathbf{F}^{-\top}$ are its transpose and inverse transpose, respectively, $\mathbf{C} \equiv \mathbf{F}^\top \cdot \mathbf{F}$ is the right Cauchy-Green deformation tensor. The choice of \mathbf{C} as a measure of the deformation guarantees that the Principle of Frame

Indifference is satisfied. $W = W(\mathbf{C})$ is the elastic potential that is defined as follows^(39,41)

$$W(\mathbf{C}) = \int_{\Sigma} R(\hat{\mathbf{M}})w(\Lambda(\mathbf{C}, \hat{\mathbf{M}})) d\Sigma, \quad (3.5)$$

where Σ is the set of all material directions in the reference configuration, $\hat{\mathbf{M}}$ is an arbitrary material direction in Σ , $R(\hat{\mathbf{M}})$ is the probability density function for collagen fibers to be aligned in the direction $\hat{\mathbf{M}}$, and $w(\Lambda(\mathbf{C}, \hat{\mathbf{M}}))$ is the elastic potential of collagen fibers in the direction $\hat{\mathbf{M}}$ determined by the axial fiber stretch

$$\Lambda(\mathbf{C}, \hat{\mathbf{M}}) = \sqrt{\hat{\mathbf{M}} \cdot \mathbf{C} \cdot \hat{\mathbf{M}}}. \quad (3.6)$$

According to (3.6), the stretch of each fiber Λ along its mean axis $\hat{\mathbf{M}}$ is derived from an affine transformation of the overall tissue's strain \mathbf{C} .

After defining the fiber elastic stress $\sigma(\Lambda)$ as

$$\sigma(\Lambda) \equiv \frac{dw(\Lambda)}{d\Lambda}, \quad (3.7)$$

the constitutive equation (3.4) takes the form

$$\mathbf{P} = -p\mathbf{F}^{-\top} + \mathbf{F} \cdot \int_{\Sigma} R(\hat{\mathbf{M}}) \frac{\hat{\mathbf{M}}\hat{\mathbf{M}}}{\Lambda(\mathbf{C}, \hat{\mathbf{M}})} \sigma(\Lambda(\mathbf{C}, \hat{\mathbf{M}})) d\Sigma. \quad (3.8)$$

Given the collagen fiber distribution $R(\hat{\mathbf{M}})$ and the fiber stress-stretch relation $\sigma(\Lambda)$ defined by (3.2)-(3.3), the constitutive law (3.8) defines the multiaxial mechanical response of the ligamentous material.

The three-dimensional model (3.8) can be reduced to the one-dimensional model (3.2)-(3.3) under certain assumptions. Assume that the ligament undergoes an isochoric axisymmetric deformation defined by the following deformation gradient

$$\mathbf{F} = \lambda^{-\frac{1}{2}} \mathbf{e}_r \mathbf{E}_R + \lambda^{-\frac{1}{2}} \mathbf{e}_\theta \mathbf{E}_\Theta + \lambda \mathbf{e}_z \mathbf{E}_Z, \quad (3.9)$$

where the λ is the axial stretch, $\{\mathbf{E}_R, \mathbf{E}_\Theta, \mathbf{E}_Z\}$ and $\{\mathbf{e}_r, \mathbf{e}_\theta, \mathbf{e}_z\}$ are orthonormal bases such that \mathbf{E}_Z and \mathbf{e}_z are unit vectors parallel to the direction of physiological loading in the reference and current configurations, respectively. Consequently, the right Cauchy-Green deformation tensor is given by

$$\mathbf{C} = \lambda^{-1} \mathbf{E}_R \mathbf{E}_R + \lambda^{-1} \mathbf{E}_\Theta \mathbf{E}_\Theta + \lambda^2 \mathbf{E}_Z \mathbf{E}_Z. \quad (3.10)$$

Moreover, assume that collagen fibers are perfectly parallel to the direction of loading so that $R(\hat{\mathbf{M}}) = \delta(\hat{\mathbf{M}} - \mathbf{E}_Z)$ where δ is the Dirac-delta function. It then follows from (3.6), (3.8), (3.9), and (3.10) that the non-zero components of the first Piola-Kirchhoff stress are

$$P_{rR} = P_{\theta\Theta} = -p\lambda^{\frac{1}{2}}, \quad P_{zZ} = -p\lambda^{-1} + \sigma(\lambda). \quad (3.11)$$

Because of the traction-free boundary condition on the lateral surface of the ligament, the indeterminate pressure term p assumes zero value. One then obtains that the only non-zero component of the stress, P_{zZ} , reduces to the axial fiber stress, σ , defined by (3.2)-(3.3).

3.3 RESULTS

In order to test the constitutive model described by (3.2)-(3.3), the number N of the collagen fibers that are assumed to form the ligament has been chosen to be 10,000 since no significant difference have been observed in the computation of the stress by increasing this number.

The straightening stretches and failure stretches for the collagen fibers have been computed by transforming uniform deviates, generated by using Park and Millers Minimal Standard generator with an additional shuffle,^(72,73) into Weibull distributed deviates.

The set of material parameters $\{K, \alpha_s, \beta_s, \alpha_f, \beta_f\}$ that appear in the model has been identified by minimizing the sum of squares difference between experimental and theoretical stresses. To this end, the Downhill Simplex Method has been numerically implemented.^(73,74) This method permits the evaluation of the minimum of a function with several independent variables without requiring the computation of its derivatives.

MCL tensile test data published by Abramowitch et al.⁽⁷⁵⁾ and by Provenzano et al.⁽⁷⁶⁾ have been employed to test the proposed constitutive model. Abramowitch and collaborators have performed uniaxial tensile tests on femur-MCL-tibia complexes to evaluate the goat as animal model for studying the MCL healing process.⁽⁷⁵⁾ They have reported a typical stress-strain data that shows the MCL tearing and complete failure. These data are well fitted by the presented model as Figure 3.3 illustrates. The model is able to describe the toe region, the linear region and, most importantly, the failure region of the stress-strain curve. The values of the parameters have been found to be $K = 460$ MPa, $\alpha_s = 1.74$, $\beta_s = 0.02$, $\alpha_f = 8.10$, and $\beta_s = 0.18$ ($R^2 = 0.99$). In Figure 3.3, the fractions of taut fibers and the fractions of broken fibers are also depicted.

As mentioned earlier, a common assumption in previous works on modeling failure in soft tissues is that the fibers, which comprise the tissues, have an identical failure stretch, defined relatively to the taut configuration^(59,66,71) (Section 3.1). By invoking this assumption, the single fiber stress takes the following form

$$\sigma^{(i)} = \begin{cases} 0 & \frac{\Lambda}{\Lambda_s^{(i)}} \leq 1 ; \\ K \left(\frac{\Lambda}{\Lambda_s^{(i)}} - 1 \right) & 1 < \frac{\Lambda}{\Lambda_s^{(i)}} < \Lambda_f ; \\ 0 & \frac{\Lambda}{\Lambda_s^{(i)}} \geq \Lambda_f , \end{cases} \quad (3.12)$$

where Λ_f is the failure fiber stretch with respect to the taut configuration and the other quantities appearing in (3.12) are defined as before (Section 3.2.1).

The proposed constitutive model is compared with a constitutive model defined by (3.12)-(3.3). It is noteworthy that, to simulate the disruption of the ligament, two parameters, α_f and β_f , are needed to randomly generate the failure fiber stretches, $\Lambda_f^{(i)}$, in the model (3.2)-(3.3) whereas one parameter, Λ_f , is needed to define the failure fiber stretch in the model (3.12)-(3.3).

Figure 3.4 presents the comparison between the curve fittings of the models described by (3.2)-(3.3) and by (3.12)-(3.3). The four best fitting parameters for the latter model have been determined to be $K = 716$ MPa, $\alpha_s = 0.89$, $\beta_s = 0.07$, $\Lambda_f = 1.16$ ($R^2 = 0.98$). As Figure 3.4 shows, the newly proposed model can fit the data better than the four parameter model (3.12)-(3.3).

Provenzano et al.⁽⁷⁶⁾ have conducted an experimental study to analyze the subfailure damage in ligament. In their study, they have subjected rat femur-MCL-tibia complexes to tensile tests in order to measure the mechanical properties of the ligament before and after applying subfailure stretches. A good agreement has been found between the proposed model and the experimental data obtained from the ligament-bone complex. Figure 3.5 displays the curve fitting of the model with the experimental data, the fractions of straight fibers and the fractions of broken fibers. The material parameters have been estimated to be $K = 1345$ MPa, $\alpha_s = 1$, $\beta_s = 0.03$, $\alpha_f = 2.47$, and $\beta_s = 0.12$ ($R^2 = 0.99$).

The constitutive model (3.12)-(3.3) has also been fitted to the experimental data published by Provenzano et al.⁽⁷⁶⁾ In Figure 3.6, the the curve-fitting is compared with the curve-fitting obtained by using the newly proposed constitutive law. The value of the four material parameters, $\{K, \alpha_s, \beta_s, \Lambda_f\}$, embodied in the model (3.12)-(3.3) could not be uniquely determined. As evidenced by the results in Figure 3.6, the proposed model reproduces better the MCL stress-stretch mechanical behavior.

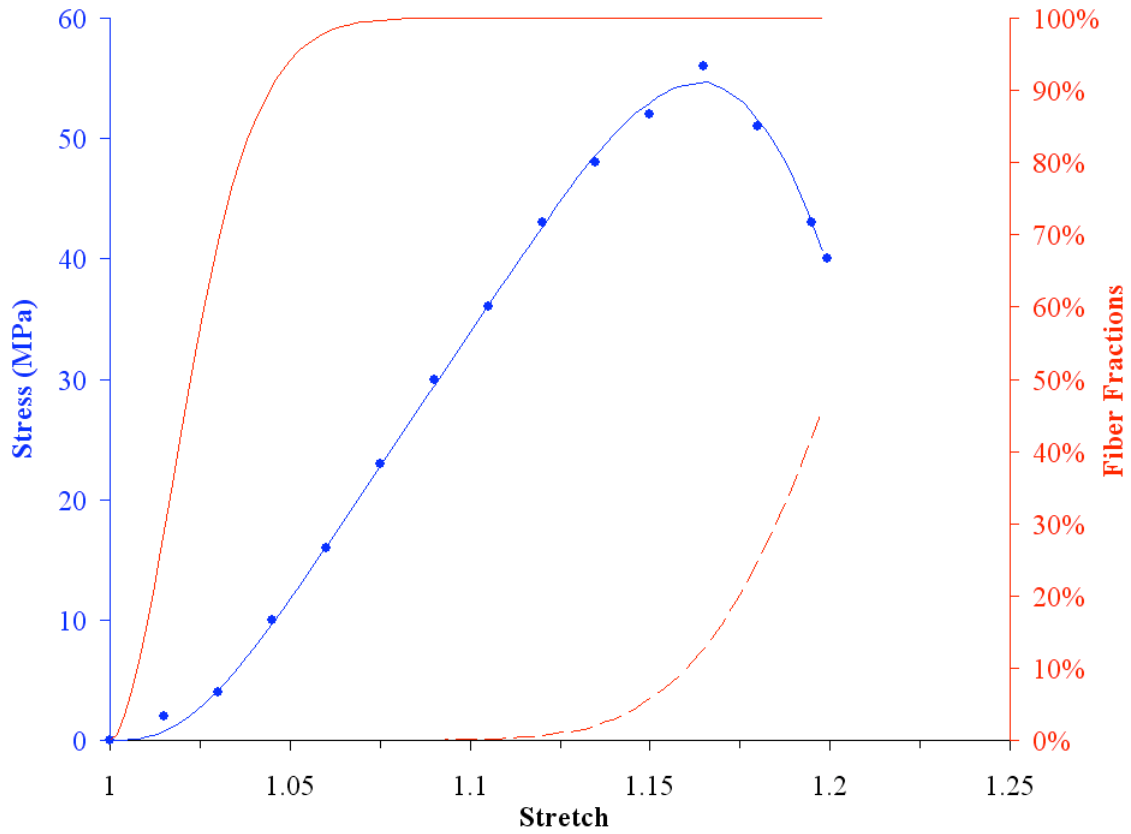


Figure 3.3. Stress-strain experimental data from Abramowitch and colleagues⁽⁷⁵⁾ (●) with model fit (—), fractions of straight fibers (—), and fractions of broken fibers (---).

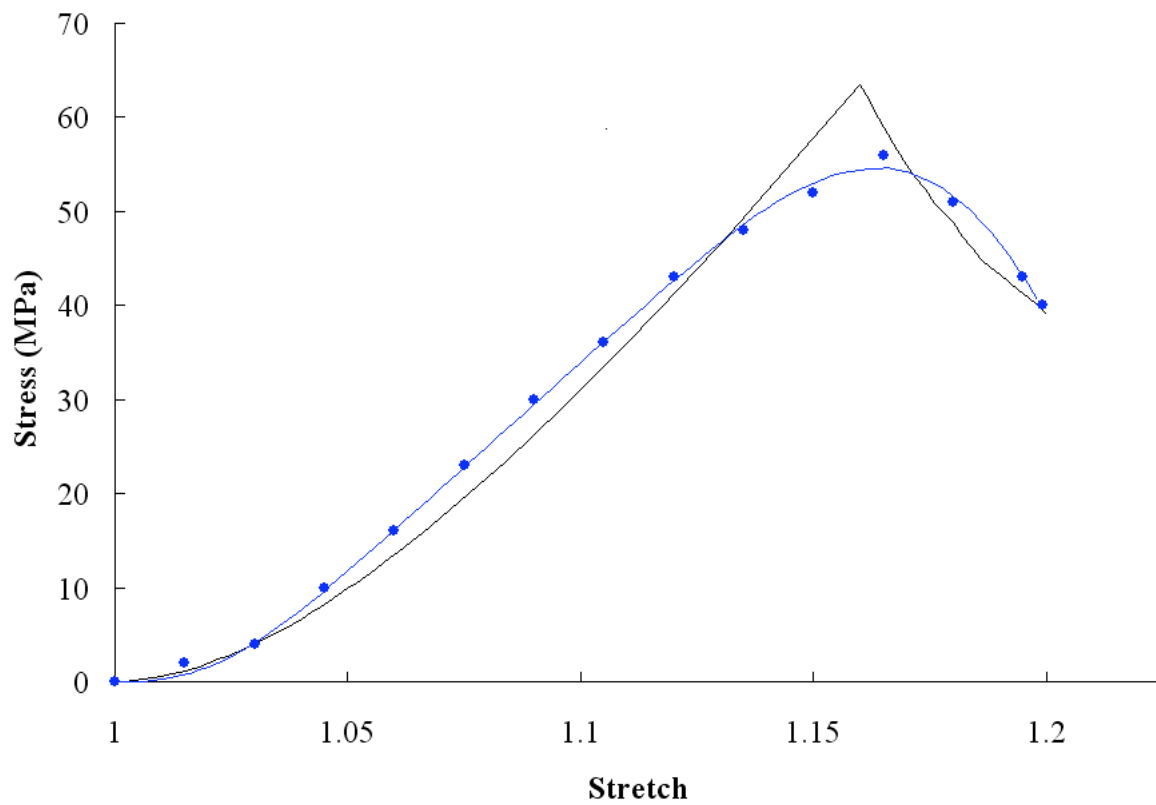


Figure 3.4. Stress-strain experimental data from Abramowitch and co-authors⁽⁷⁵⁾ (●) with five parameter model fit (—) and four parameter model fit (—).

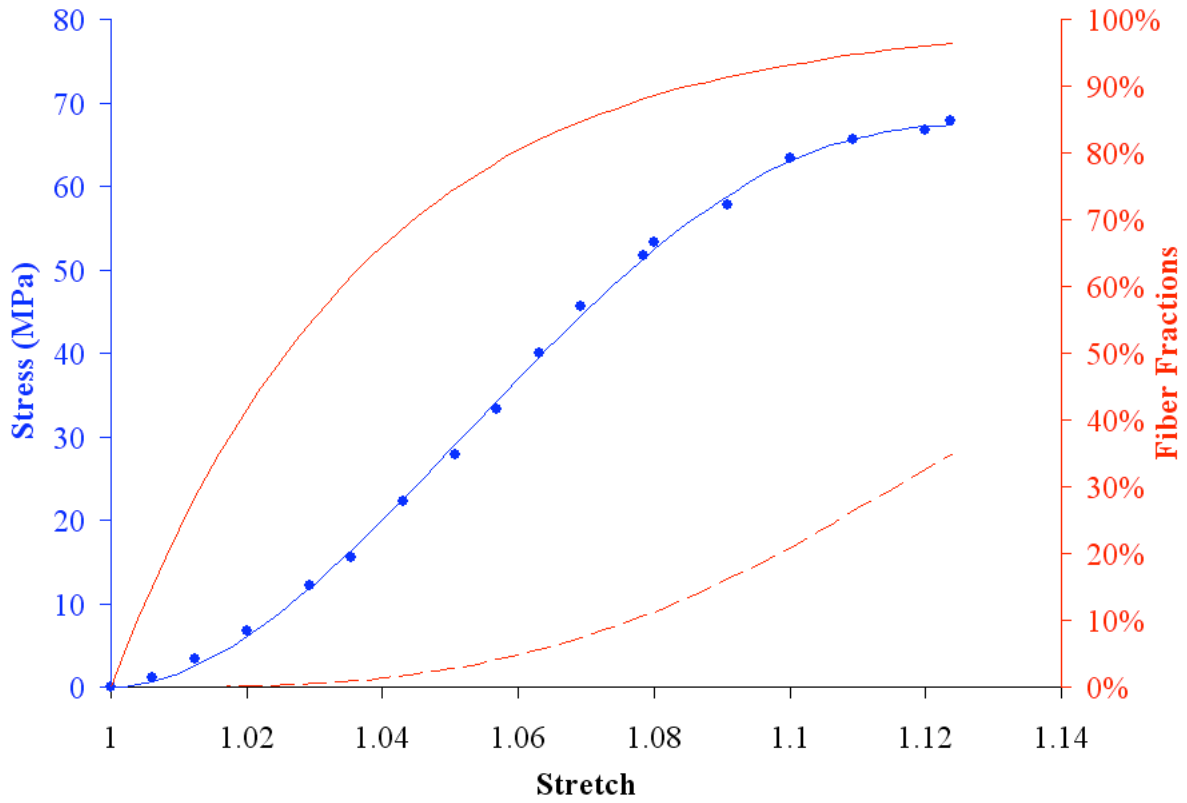


Figure 3.5. Stress-strain experimental data from Provenzano et al.⁽⁷⁶⁾ (●) with model fit (—), fractions of straight fibers (—), and fractions of broken fibers (---).

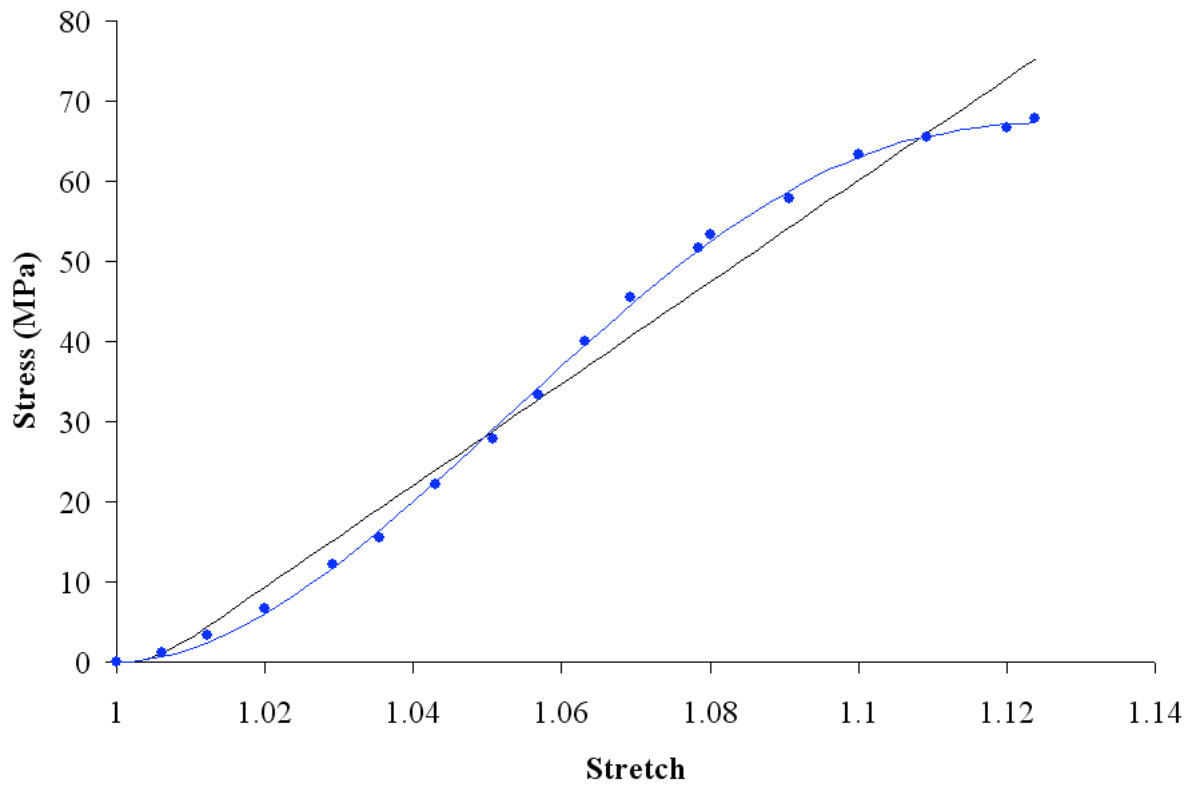


Figure 3.6. Stress-strain experimental data from Provenzano et al.⁽⁷⁶⁾ (●) with five parameter model fit (—) and four parameter model fit (—).

3.4 DISCUSSION

A novel structural constitutive model for the description of the tensile behavior of knee ligaments is presented. The model is formulated by assuming that the ligament is composed of undulated collagen fibers that are straighten out upon stretching. They are assumed to bear load only after losing their waviness and until they rupture. The recruitment and the disruption of collagen fibers are defined by statistical distributions. The model is capable to properly reproduce the toe region, the linear region, and the failure region of stress-strain curves of MCLs reported in published experimental studies.^(75,76) Furthermore, an extension to a three-dimensional material law is formulated within the context of structural mechanics for soft tissues.^(39,41)

The good agreement between the proposed constitutive model and the uniaxial experimental data published by Abramowitch et al.⁽⁷⁵⁾ and Provenzano et al.⁽⁷⁶⁾ confirms the utility of the model in describing the process leading to partial and complete rupture of ligamentous tissues. The five parameters, which appear in the model, are sufficient to illustrate the tensile behavior of these tissues. Since the model is structurally-based, these parameters provide insight into the relation between the histology and the mechanics of the tissues. The estimated stiffness constants of the collagen fiber for the goat and rat MCLs are within the stiffness range reported in the biomechanical literature.^(9,60,66) The remaining parameters permits the determination of the percentages of taut and broken fibers at each value of the tissue's stretch.

The tensile properties of the goat MCL are related to the recruitment and failure of collagen fibers in Figure 3.3. It can be seen that the percentage of straight fibers increases gradually with stretch in the toe region of the stress-stretch curve. The fibers are taut and contribute to the overall tissue's stress in the linear region of the curve. Finally, the ligament is torn when 46% of the collagen fibers fail as shown in Figure 3.3.

The rat MCL stress-stretch data reported by Provenzano et al.⁽⁷⁶⁾ are characterized by the absence of a distinct linear region (See Figure 3.5). For this reason, the constitutive model predicts that the ligament experiences a complete rupture when 96% of the collagen fibers are recruited to bear load and 35% of such fibers fail. This suggests that some collagen fibers remain crimped when the ligament breaks.

The stress of knee ligaments exhibited either an abrupt or a gradual drop in the failure region of the stress-strain experimental data. Liao and Belkoff speculated that this difference in the failure regime is age-related.⁽⁶⁶⁾ In their study on rabbits, they found that the 4-month-old MCLs exhibit a prolonged failure region whereas the 7-month-old MCLs exhibit an abrupt failure region. However, the cause of the different shapes of the stress-strain curves is unclear and can be ascribed to numerous factors that include experimental methodologies and animal model age, species, and sex.

The proposed model provides a better fit to the experimental data than the model formulated by assuming that the straight fibers in the ligamentous specimen have an identical failure stretch (See Figure 3.4 and Figure 3.6). It needs to be noted that the model presented herein is akin to the model proposed by Wren and Carter⁽⁷¹⁾ in the definitions of fiber stress and tissue's stress. In their formulation, soft tissues are viewed as composite materials in which both the fibers and the ground substance are assumed to contribute to the tissues' mechanical response. Moreover, these investigators introduced into their model the fiber volume fraction, the fiber orientation and the resistance of the ground substance to the fiber reorientation. However, the values of the parameters in the model were inferred from different experimental studies in order to simulate the nonlinear stress-strain relationship of soft skeletal connective tissues.

Recent studies have revealed that the crimp period of collagen fibrils in rabbit MCLs is location-dependent.⁽⁷⁷⁾ These inhomogeneities seem to suggest that the gross constitutive behavior of these ligaments must be derived by taking into consideration their fibrillar structure. Hurscheler and associates⁽⁵⁹⁾ developed a model for ligaments and tendons incor-

porating the structure of the tissues both at the fiber level and at the fibril level. However, their model could not be completely validated since the microstructural information, which is required for the determination of the material parameters, was not available.

In order to account for the anisotropic material behavior of MCLs, a three-dimensional model is also formulated. The one-dimensional model is generalized by adopting the Lanir's structural approach.^(39,41) The anisotropy of the tissue is modeled by introducing a statistical distribution for the collagen fiber orientation. However, the three-dimensional constitutive model is not assessed since multiaxial mechanical tests complemented with quantification of the collagen fiber orientation are needed.

While the model demonstrated that the collagen fiber alone is responsible for the mechanical behavior of the ligamentous tissue, it does not address other factors which concur to determine the failure properties of these tissue. The fluid-dominated ground substance influences the mechanics of the ligaments. However, little is known about its role in the failure mechanisms. Furthermore, because the stress-strain curves of the rat MCLs have been observed to change after a critical subfailure stretch along their directions of physiological loading,⁽⁷⁶⁾ it is speculated that damage of individual collagen fiber occurs during injury. A structural constitutive model, which accounts for damage of knee ligaments, will be the focus of future research.

4.0 FUTURE DIRECTIONS: A STRUCTURAL MODEL FOR THE SUBFAILURE DAMAGE

Some preliminary results on constitutive modeling for the description of the subfailure damage behavior of knee ligaments are presented hereafter. It needs to be emphasized that these findings are not conclusive but they rather suggest future areas of investigations.

4.1 SUBFAILURE DAMAGE IN KNEE LIGAMENTS

While the third-degree sprain is the most severe pathology of the knee ligaments, the first-degree sprain and second-degree sprain are the most common. Epidemiological studies have estimated that more than 85% of the ligamentous injuries consist of first-degree and second-degree sprains.⁽⁷⁸⁾ In first-degree sprains, the ligament is overly stretched and microscopically damaged. Second-degree sprains involve the partial tearing of the ligament. The treatment for both injuries is usually non-operative. Despite the high incidence, few experimental studies^(76,79,80) have been directed to analyze the change in the mechanical properties of knee ligaments when microtrauma and partial tears occur.

Second-degree sprains were first mechanically studied by Laws and Walton in sheep MCLs.⁽⁷⁹⁾ It was demonstrated that the tensile strength of the ligament decreased by 13% immediately after the injury but it returned to its normal value after six weeks. Moreover, the laxity of the knee was observed to increase post-injury.

Some researchers investigated the influence of subfailure injuries on the mechanical properties of rabbit ACLs.⁽⁸⁰⁾ Briefly, paired ACLs were used to evaluate the tensile properties of the ligaments subjected to subfailure injuries. The subfailure injury of each ligament was

defined as 80% of the ultimate deformation of the paired control ligament. The ultimate load, ultimate deformation and energy absorbed at failure were seen not to change profoundly following the subfailure stretch. However, the shape of the load-deformation curve was noted to be remarkably different: the deformations measured at 5%, 10%, 25%, and 50% of the failure load and the stiffness computed at 50% of the failure load were greater for the ACLs subjected to the subfailure injuries than for the ACLs in the control group. The major changes were observed in the toe region of the load-deformation and were correlated to the increased laxity of the knee joint.⁽⁸⁰⁾

The most comprehensive study of subfailure damage has been conducted on rat MCLs by Provenzano and co-authors.⁽⁷⁶⁾ The structural damage was defined as the nonrecoverable difference in the ligament length after subfailure stretches. The authors reported that the length of the MCLs permanently increased after subfailure strains that were greater than 5.14%. Moreover, they analyzed the effects of different subfailure stretches on the stress-strain relation of the rat MCLs. In particular, they performed uniaxial tensile tests on twelve tibia-MCL-femur complexes from six animals along the longitudinal axes of the ligaments. Six MCLs, each from one of the six animals, were used as control and were pulled to failure. The contralateral ligaments were subjected to displacement controlled tests with subfailure strains of 0%, 4.7%, 5.1%, 6%, 7%, and 9%. In particular, each MCL was preconditioned and it was allowed to recover in order to eliminate possible creep effects. After recovery, the MCL was preloaded up to the subfailure stretch, then unloaded and allowed to recover again. Subsequently, the MCL was reloaded until complete rupture occurred. The stress-strain responses of the MCLs were observed to change during the second loading when the subfailure stretches in the first loading exceeded the damage threshold corresponding to 5.14% strain. The toe region of the stress-strain curve was noted to be elongated while the tangent modulus and the tensile strength were found to decrease with increasing subfailure strain.

Motivated by the work of Provenzano and colleagues,⁽⁷⁶⁾ a constitutive relation is proposed in an attempt to capture the effects of subfailure damage on the mechanical properties of the knee ligaments. Similar to the constitutive models, which have been presented in Chapter 2 and Chapter 3, the model is formulated under the assumption that collagen is the only load-bearing component of the ligamentous tissue. The gross damage of the tissue is assumed to be determined by the damage of individual collagen fibers. Preliminary results obtained by curve fitting the model to the experimental data published by Provenzano et al.⁽⁷⁶⁾ are reported. The predictive capability of the model are investigated and the model limitations are discussed.

4.2 MODEL FORMULATION

The ligament is assumed to be composed of N collagenous fibers, which run parallel to the in vivo loading direction, where N denotes an integer—elastin and fluid-like matrix are disregarded. The collagen fibers are crimped in the slack configuration. They are straighten out under deformation and start to bear load after becoming straight.

The straightening stretches for the N fibers are assumed to be randomly distributed according to a Weibull cumulative distribution. Let $\Lambda_s^{(i)}$ denote the straightening stretch of the collagen fiber i , where $i = 1 \dots N$. It follows that

$$\Lambda_s^{(i)} = 1 + \beta_s [\ln(1 - G^{(i)})]^{-\frac{1}{\alpha_s}}, \quad (4.1)$$

where $G^{(i)}$ is a random number satisfying $0 < G^{(i)} < 1$, $\alpha > 0$ is the shape parameter and $\beta > 0$ is the scale parameter of the Weibull distribution.

The collagenous fiber behaves as a linear elastic material with stiffness K_1 up to damage. It is postulated that the individual fiber is damaged at a threshold stretch Λ_d and it breaks at a threshold stretch Λ_f with $\Lambda_f > \Lambda_d$. Both stretches, Λ_f and Λ_d , are defined with respect

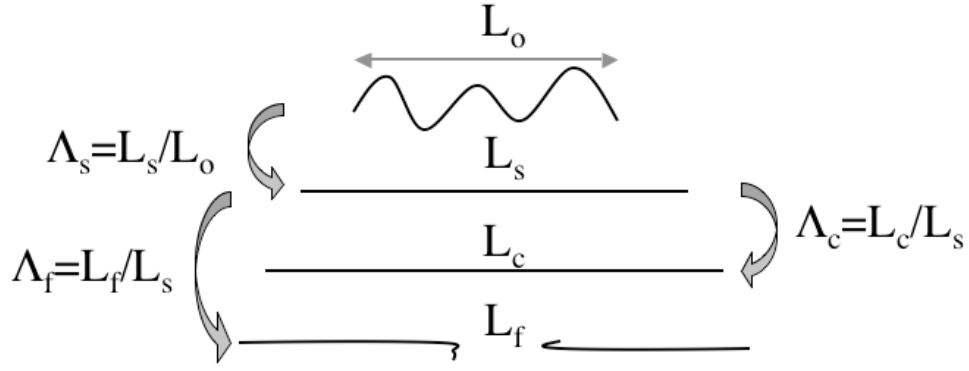


Figure 4.1. Λ_s : straightening fiber stretch. Λ_d : damage fiber stretch. Λ_f : failure fiber stretch.

to the taut configuration (See Figure 4.1). Damage of the collagen fiber i is defined as a reduction of the stiffness K_1 by a factor $D^{(i)}$ given by

$$D^{(i)} = 1 - \frac{\frac{\Lambda}{\Lambda_s^{(i)}} - \Lambda_d}{\Lambda_f - \Lambda_d} = \frac{\Lambda_f - \frac{\Lambda}{\Lambda_s^{(i)}}}{\Lambda_f - \Lambda_d}, \quad (4.2)$$

with $\Lambda_d < \frac{\Lambda}{\Lambda_s^{(i)}} < \Lambda_f$. It is worth noting that the damage parameter $D^{(i)}$ satisfies $D^{(i)} \rightarrow 0$ when $\frac{\Lambda}{\Lambda_s^{(i)}} \rightarrow \Lambda_f^-$ and $D^{(i)} \rightarrow 1$ when $\frac{\Lambda}{\Lambda_s^{(i)}} \rightarrow \Lambda_d^+$. Moreover, when the fiber completely fails, it becomes unable to support load. Thus, the stress, $\sigma^{(i)}$, for a generic fiber i takes the form

$$\sigma^{(i)} = \begin{cases} 0 & \frac{\Lambda}{\Lambda_s^{(i)}} < 1 ; \\ K_1 \left(\frac{\Lambda}{\Lambda_s^{(i)}} - 1 \right) & 1 < \frac{\Lambda}{\Lambda_s^{(i)}} \leq \Lambda_d ; \\ D^{(i)} K_1 \left(\frac{\Lambda}{\Lambda_s^{(i)}} - 1 \right) & \Lambda_d < \frac{\Lambda}{\Lambda_s^{(i)}} < \Lambda_f ; \\ 0 & \frac{\Lambda}{\Lambda_s^{(i)}} \geq \Lambda_f , \end{cases} \quad (4.3)$$

where Λ is the overall tissue's stretch and $\Lambda/\Lambda_s^{(i)}$ is the fiber stretch relative to the taut configuration (See Figure 4.2).

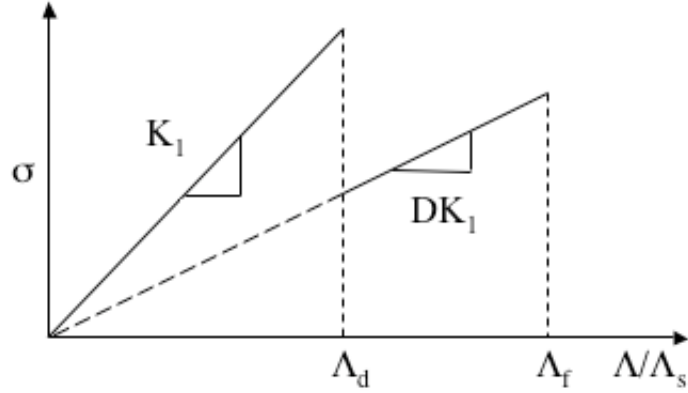


Figure 4.2. Fiber stress-stretch relation.

The overall tissue's stress, σ , is computed by averaging the stresses, $\sigma^{(i)}$, of the N collagen fibers. Thus, it is given by

$$\sigma(\Lambda) = \frac{1}{N} \sum_{i=1}^N \sigma^{(i)}. \quad (4.4)$$

A set of five structural parameters, $\{K, \alpha, \beta, \Lambda_f, \Lambda_d\}$, needs to be determined in order to replicate the typical stress-stretch relationship of ligaments. It needs to be remarked that the model given by (4.3)-(4.4) can be generalized to a three-dimensional constitutive law by following the same arguments as in Section 3.2.2.

4.3 PRELIMINARY RESULTS

The constitutive model has been applied to experimental data acquired by performing uniaxial tensile tests on a pair of femur-MCL-tibia complexes.⁽⁷⁶⁾ One of the two femur-MCL-tibia complexes was pulled to failure and used as control in order to study the changes in the mechanical properties of the ligament due to the subfailure damage. The other femur-MCL-tibia complex was stretched to a peak value $\Lambda_p = 1.09$. It was unloaded and, after a recovery time that assured the absence of creep behaviors, it was re-stretched until the femur-MCL-tibia was completely ruptured.

The sum of the squares difference between experimental and theoretical stresses has been minimized to find the values of the material parameters, which are embodied in the proposed model, by using the Downhill Simplex Method.^(73,74) The model (4.3)-(4.4) has been numerically implemented by using $N = 10,000$ collagen fibers. Furthermore, as described in Section 3.3, uniform deviates have been transformed into Weibull deviates to generate the straightening stretches for the N fibers.^(72,73)

The experimental data obtained from the control femur-MCL-tibia specimen have been used to compute the four parameters $\{K, \alpha, \beta, \Lambda_f\}$. The damage stretch for the collagen fiber, Λ_d , is assumed to be equal to the threshold damage stretch of the ligamentous tissue, as experimentally determined by Provenzano et al.,⁽⁷⁶⁾ i.e. $\Lambda_d = 1.0514$. This assumption implies that the gross tissue's stretch, at which the single collagen fiber experiences damage, cannot be smaller than 1.0514. Figure 4.3 illustrates the goodness of the fit to the empirical data by the model (4.3)-(4.4). The best fit material constants have been determined to be $K = 1467$ MPa, $\alpha = 0.86$, $\beta = 0.05$, $\Lambda_f = 1.7$ ($R^2 = 0.99$). These parameters have been used to predict the mechanical response exhibited by the femur-MCL-tibia sample following the subfailure peak stretch Λ_p . Toward this end, it is noted that only the collagen fibers that do not break when the ligament is first stretched up to Λ_p contribute to carry load. In the framework of the model, fiber damage is assumed to accumulate when the ligament is re-stretched and, hence, the stiffness of the collagen fiber changes to a value K_2 given by

$$K_2 = \begin{cases} K_1 & \frac{\Lambda_p}{\Lambda_s^{(i)}} \leq \Lambda_d; \\ K_1 \left(\frac{\Lambda_f - \frac{\Lambda_p}{\Lambda_s^{(i)}}}{\Lambda_f - \Lambda_d} \right) & \Lambda_d < \frac{\Lambda_p}{\Lambda_s^{(i)}} < \Lambda_f; \\ 0 & \frac{\Lambda_p}{\Lambda_s^{(i)}} \geq \Lambda_f. \end{cases} \quad (4.5)$$

The prediction of the model at the best fitting parameters is shown in Figure 4.3. The tensile strength of the re-stretched ligament is clearly overestimated and the toe region is not well reproduced by the model prediction.

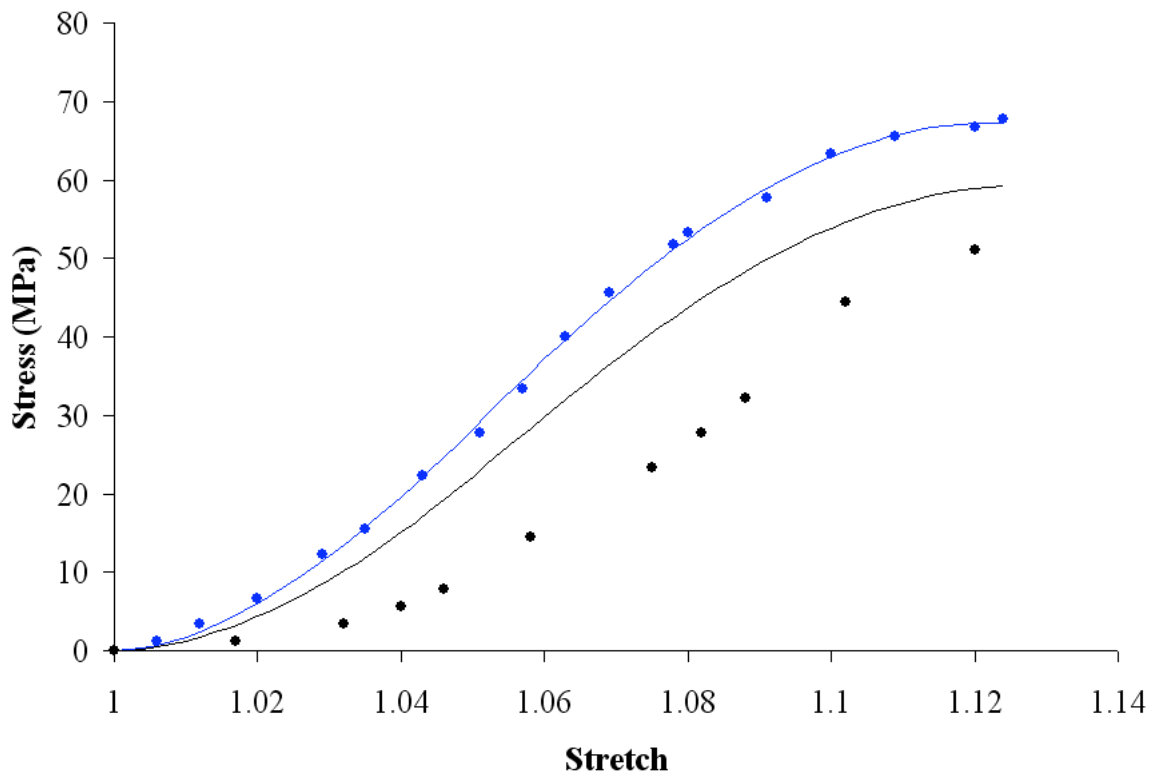


Figure 4.3. Stress-stretch curves for the control rat MCL (●) and for the re-stretched rat MCL after the peak subfailure stretch $\Lambda_p = 1.09$.⁽⁷⁶⁾ Model fit (—) and model prediction (—) are represented at best fitting parameters.

4.4 DISCUSSION

A preliminary constitutive model is presented in an attempt to describe the subfailure damage behavior in ligamentous tissues. The mechanical behavior of the tissues is determined by assembling the mechanical contributions of collagen fibers. The fibers are crimped in the slack configuration and they lose their undulation upon deformation. They contribute to the overall tissues' stress after becoming taut. The fiber straightening process is governed by a Weibull distribution. The fibers are thought to be linearly elastic, to experience damage and complete failure. The model is fitted to the experimental data for rat MCLs presented by Provenzano et al.⁽⁷⁶⁾ and its predictions are evaluated.

As graphically illustrated in Figure 4.3, the model presented provides a very good fit to the experimental data in a nonlinear least-square sense. While the value of stiffness constant $K = 1467$ MPa falls within the ranges of values reported in the biomechanical literature,^(9,66) the value of the failure stretch of the collagen fiber $\Lambda_f = 1.7$, is physically unrealistic. It suggests that the fibers do not break, although the ligament is torn. One must note that, in order to determine the material parameters of the model, the damage stretch for the collagen fibers was assumed to coincide with the gross MCL damage stretch that was computed in the experimental studies.⁽⁷⁶⁾ Nevertheless, it is reasonable to believe that the collagen fibers are damaged at a smaller stretch than the damage stretch of the ligament. This assumption, which was forced by the lack of information on the failure of the single collagen fiber, may have affected the value of Λ_f .

The predictive capabilities of the model are also investigated in order to gain an understanding of subfailure damage in ligaments. The model is able to predict the drop in tensile strength of the MCL after damage in agreement with the experimental studies.^(76,79,80) However, the predicted tensile strength is overestimated. Moreover, the model does not forecast the prolonged toe region in the stress-strain curve of ligament post-injury. The changes in the toe region, which is the region where the ligament operates during normal activity, are

important to explain the increased laxity of the knee after first- and second-degree sprains⁽⁸⁰⁾ and, therefore, need to be accurately reproduced by a constitutive model.

According to the model, the subfailure damage of the ligament results from the reduction in stiffness of the collagen fibers. The decrease in stiffness of the individual fiber can be attributed to cracking inside the fiber. Nevertheless, the form of the reduction parameter (4.2) is arbitrary and it is not inferred from micro-structural considerations. Perhaps, the constitutive relation for the mechanical characterization of subfailure damage needs to be formulated by accounting for the various structural hierarchical levels of the ligament. The dearth of information on the relation between morphology and mechanics remains the main impediment to the development of such micro-structural models for ligaments.

The outcome of this preliminary study seems to indicate that the material properties of the ligamentous tissues post-injury depend also on collagen inter-molecular and inter-fibrillar cross-linking. Collagen fiber damage and failure alone cannot explain the changes in the stress-strain curves of the normal and injured knee ligaments. In fact, the collagen inter-molecular cross-linking has been shown to affect the mechanical response of the collagen fibril. In particular, the stiffness of the cross-link-deficient collagen has been found to be lower than the stiffness of the normal collagen fibril.⁽⁸¹⁾ Additionally, the inter-fibrillar cross-links, which are established by the proteoglycan-rich matrix, may play an important role in delineating the mechanics of collagen fibrils. By performing synchrotron x-ray scattering experiments, Fratzl et al.⁽⁸²⁾ observed that the strain in the collagen fibril was 40% lower than the macroscopic strain in rat tail tendons. This difference suggested that the matrix of proteoglycan also experiences deformation. Thus, incorporating the contributions of collagen cross-linking and proteoglycan-rich matrix in the constitutive model for the subfailure damage behavior of ligaments will be the object of future studies.

5.0 CONCLUSIONS

Structural constitutive models have been presented to illustrate the strain rate dependent behavior and the mechanical failure of knee ligaments. The constitutive relations also account for the anisotropy, the nonlinearity, and the incompressibility of the ligamentous tissues. Published uniaxial tensile data^(26,28,75,76) have been used to assess the models. To this end, the ligaments are assumed to possess a perfectly parallel collagen structure and to undergo an isochoric, axisymmetric deformation. The agreement of the models with the cited empirical observations on knee ligaments is very good. The material constants, embodied in the models, are physically meaningful and, therefore, they permit to shed light on the connection between the morphology and the mechanics of these tissues.

Although the results of the proposed models are very promising, multiaxial experimental data and quantification of the collagen fiber orientation are required for their complete validation. The mechanical properties of the knee ligaments are commonly investigated by performing uniaxial tensile tests along their physiological loading direction. However, it is well known that these tissues experience complex multiaxial deformations *in vivo*.⁽⁵⁾ Therefore, the ligaments should be tested under quasi-static and dynamic loading conditions that combine compression, extension, torsion, shear, and bending. Thus, it is incumbent upon experts in experimental mechanics to fully evaluate the mechanical properties of the ligaments.

Because the present models are formulated by considering the structural architecture of the ligamentous tissues, they require detailed histological data. The collagen fiber crimping, which is incorporated into the models, could be determined by using optical coherence tomography (OCT). By using this imaging technique, Hansen and collaborators measured

the changes in crimp as a function of the applied tensile strain in fascicles of the rat tail tendon.⁽¹⁸⁾ Moreover, the angular distributions of collagen fibers, which is needed by the proposed models to account for the anisotropy of knee ligaments, could be quantified by using small angle light scattering (SALS).⁽⁴⁸⁾ Sacks and his associates^(45–47) employed this technique to identify the orientation distributions of collagen fibers in planar soft tissues and integrated the results in structural constitutive models. For non-planar tissues such as knee ligaments, aligned serial histological sections could be used to collect SALS data. By integrating the data from each section, complete information on the collagen fiber orientation in the ligaments could be acquired.⁽⁶⁷⁾

Experimental studies need to be designed to discriminate the mechanical response of the ligament's components. To this end, the ground substance could be removed from the ligamentous material by employing enzymes or chelating agents whereas the elastin could be removed by using formic acids as presented in early studies by Minns and colleagues.⁽³³⁾ The ligamentous tissue could be mechanically tested under various loading conditions before and after being subjected to these chemical treatments. The findings obtained could clarify the role of the elastin and ground substance on the overall mechanical behavior of ligaments. Recently, Bonifasi-Lista et al.⁽¹⁶⁾ conducted transverse tensile tests and shear tests along the fiber direction of MCLs and gained insight on the mechanical function of inter-molecular or/and inter-fibrillar cross-links. Because the cross-links are primarily oriented orthogonally to the direction of the molecules and fibrils, the authors speculated that such tests could be useful to determine the inter-molecular or/and inter-fibrillar cross-linking effects on the elastic and viscoelastic properties of the ligaments. Similar experiments should be performed in conjunction with chemical treatments that isolate the various constituents of the ligamentous tissue in order to acquire information on the relationship between the mechanical and the structural features.

In closing, robust structural constitutive models for knee ligaments can help in clarifying the roles of their constituents in determining their macroscopic mechanical response. The

models can assist at designing suitable mechanical and histological experiments that discern the mechanical behavior of collagen, elastin, and proteoglycan-rich matrix as exhibited during injuries. Moreover, they can promote the understanding of ligament mechanics when experiments are too complex and costly to be performed.

BIBLIOGRAPHY

1. S. Bollen. Epidemiology of knee injuries: diagnosis and triage. *British Journal of Sports Medicine*, 34(3):227–228, 2000.
2. M. Lafferty and S. Panella. *A.D.A.M. interactive anatomy student lab guide*. Benjamin/Cummings Publishing, Menlo Park, California, 1999.
3. A. B. Wilson and W. N. Scott. Anterior cruciate ligament. In A. J. Tria, Jr., editor, *The Ligaments of the Knee*, pages 159–184. Raven Press, 1995.
4. C. T. Laurencin, A. M. A. Ambrosio, M. D. Borden, and J. A. Cooper Jr. Tissue engineering: Orthopedic applications. *Annual Review of Biomedical Engineering*, 1:19–46, 1999.
5. J. A. Weiss and J. C. Gardiner. Computational modeling of ligament mechanics. *Critical Review in Biomedical Engineering*, 29:1–70, 2001.
6. C. Truesdell and W. Noll. *The Non-Linear Field Theories of Mechanics*. Springer-Verlag, 1965.
7. W. M. Becker, L. J. Kleinsmith, and J. Hardin. *The World of the Cell*. Benjamin/Cummings Publishing, San Francisco, 2003.
8. D. Amiel, E. Billings, Jr., and W. H. Akeson. Ligament structure, chemistry, and physiology. In D. M. Daniel, W. H. Akeson, and J. J. O’ Connor, editors, *Knee Ligaments: Structure, Function, Injury and Repair*, pages 77–91. Raven Press, New-York, 1990.
9. Y. C. Fung. *Biomechanics: Mechanical Properties of Living Tissues*. Springer-Verlag, New York, 1993.
10. A. Viidik. Structure and function of normal and healing tendons and ligaments. In V. C. Mow, M. Ratcliffe, and S. L. Y. Woo, editors, *Biomechanics of Diarthrodial Joints*, volume 1, pages 3–38. Springer-Verlag, New-York, 1990.
11. M. Comninou and I. V. Yannas. Dependence of stress-strain nonlinearity of connective tissues on the geometry of collagen fibers. *Journal of Biomechanics*, 9:427–433, 1976.
12. J. Diamant, A. Keller, E. Baer, M. Litt, and R. G. C. Arridge. Collagen; ultrastructure and its relation to mechanical properties as a function of ageing. *Proceedings of the Royal Society of London*, 180B:293–315, 1972.

13. J. Kastelic, A. Galeski, and E. Baer. The multicomposite structure of tendon. *Connective Tissues Research*, 6:11–23, 1978.
14. C. Hurschler, P. P. Provenzano, and R. Vanderby, Jr. Scanning electron microscopic characterization of healing and normal rat ligament microstructure under slack and loaded conditions. *Connective Tissue Research*, 44:59–68, 2003.
15. K. M. Quapp and J. A. Weiss. Material characterization of human medial collateral ligament. *Journal of Biomechanical Engineering*, 120:757–763, 1998.
16. C. Bonifasi-Lista, S. P. Lake, M. S. Small, and J. A. Weiss. Viscoelastic properties of the human medial collateral ligament under longitudinal, transverse and shear loading. *Journal of Orthopaedic Research*, 23:67–76, 2005.
17. A. Viidik and R. Ekholm. Light and electron microscopic studies of collagen fibers under strain. *Z Anat Entwickl Gesch*, 127:154–164, 1968.
18. K. A. Hansen, J. A. Weiss, and J. K. Barton. Recruitment of tendon crimp with applied tensile strain. *Journal of Biomechanical Engineering*, 124:72–77, 2002.
19. S. L. Y. Woo, J. A. Weiss, and D. A. MacKenna. Biomechanics and morphology of the medial collateral and anterior cruciate ligaments. In V. C. Mow, M. Ratcliffe, and S. L. Y. Woo, editors, *Biomechanics of Diarthrodial Joints*, volume 1, pages 63–104. Springer-Verlag, New-York, 1990.
20. S. L. Y. Woo, K. J. Ohland, and J. A. Weiss. Aging and sex-related changes in the biomechanical properties of the rabbit medial collateral ligament. *Mechanisms of Aging and Development*, 56:129–142, 1990.
21. R. P. Hubbard and K. J. Chun. Mechanical responses of tendons to repeated extensions and wait periods. *Journal of Biomechanical Engineering*, 110:11–19, 1988.
22. B. K. Graf, R. Vanderby, Jr., M. J. Ulm, R. P. Rogalski, and R. J. Thielke. Effects of preconditioning on the viscoelastic response of primate patella tendon. *Arthroscopy*, 10:90–96, 1994.
23. A. Sverdlik and Y. Lanir. Time-dependent mechanical behavior of sheep digital tendons, including the effects of preconditioning. *Journal of Biomechanical Engineering*, 124:78–84, 2002.
24. S. L. Y. Woo, R. H. Peterson, K. J. Ohland, T. J. Sites, and M. I. Danto. The effects of strain rate on the properties of the medial collateral ligament in skeletally immature and mature rabbits: A biomechanical and histological study. *Journal of Orthopaedic Research*, 8:712–721, 1990.
25. D. P. Pioletti, L. R. Rakotomanana, J. F. Benvenuti, and P. K. Leyvraz. Viscoelastic constitutive law in large deformations: application to human knee ligaments and tendons. *Journal of Biomechanics*, 31:753–757, 1998.

26. D. P. Pioletti, Rakotomanana, L. R., and P. K. Leyvraz. Strain rate effect on the mechanical behavior of the anterior cruciate ligament-bone complex. *Medical Engineering & Physics*, 21:95–100, 1999.
27. J. A. Weiss, J. C. Gardiner, and C. Bonifasi-Lista. Ligament material behavior is non-linear, viscoelastic and rate-independent under shear loading. *Journal of Biomechanics*, 35:943–950, 2002.
28. M. I. Danto, Woo, and S. L. Y. The mechanical properties of skeletally mature rabbit anterior cruciate ligament and patellar tendon over a range of strain rates. *Journal of Orthopaedic Research*, 11:58–67, 1993.
29. S. L. Y. Woo, M. A. Gomez, and W. H. Akeson. The time and history-dependent viscoelastic properties of the canine medial collateral ligament. *Journal of Biomechanical Engineering*, 103:293–298, 1981.
30. S. L. Y. Woo. Mechanical properties of tendons and ligaments I. quasi-static and non-linear viscoelastic properties. *Biorheology*, 19:385–396, 1982.
31. G. M. Thornton, A. Oliynyk, C. B. Frank, and N. G. Shrive. Ligament creep cannot be predicted from stress relaxation at low stress: A biomechanical study of the rabbit medial collateral ligament. *Journal of Orthopaedic Research*, 15:652–656, 1997.
32. P. Provenzano, R. Lakes, T. Keenan, and R. Vanderby. Nonlinear ligament viscoelasticity. *Biomedical Engineering Society*, 29:908–914, 2001.
33. R. J. Minns, P. D. Soden, and D. S. Jackson. The role of the fibrous components and ground substance in the mechanical properties of biological tissues: a preliminary investigation. *Journal of Biomechanics*, 6:153–165, 1973.
34. D. Chimich, N. Shrive, C. Frank, L. Marchuk, and R. Bray. Water content alters viscoelastic behaviour of the normal adolescent rabbit medial collateral ligament. *Journal of Biomechanics*, 25:831–7, 1992.
35. M. Frisen, M. Magi, L. Sonnerup, and A. Viidik. Rheological analysis of soft collagenous tissues-Part I: Theoretical considerations. *Journal of Biomechanics*, 2:13–20, 1969.
36. D. C. Stouffer, D. L. Butler, and D. Hosny. The relationship between crimp pattern and mechanical response of human patellar tendon-bone units. *Journal of Biomechanical Engineering*, 107:158–65, 1985.
37. W. F. Decraemer, M. A. Maes, V. J. Vanhuyse, and P. Vanpeperstraete. A non-linear viscoelastic constitutive equation for soft biological tissues based upon a structural model. *Journal of Biomechanics*, 13:559–564, 1980.
38. J. Kastelic, I. Palley, and E. Baer. A structural mechanical model for tendon crimping. *Journal of Biomechanics*, 13:887–893, 1980.

39. Y. Lanir. A structural theory for the homogeneous biaxial stress-strain relationship in flat collagenous tissues. *Journal of Biomechanics*, 12:423–436, 1979.
40. Y. Lanir. A microstructural model for the rheology of mammalian tendon. *Journal of Biomechanical Engineering*, 102:332–339, 1980.
41. Y. Lanir. Constitutive equations for fibrous connective tissues. *Journal of Biomechanics*, 16:1–12, 1983.
42. T. T. Soong and W. N. Huang. A stochastic model for biological tissue elasticity in simple elongation. *Journal of Biomechanics*, 6:451–458, 1973.
43. A. Horowitz, Y. Lanir, F. C. P. Yin, M. Perl, I. Sheinman, and R. K. Strumpf. Structural three-dimensional constitutive law for the passive myocardium. *Journal of Biomechanical Engineering*, 110:200–207, 1988.
44. P. Zioupos and Barbenel J. C. Mechanics of native bovine pericardium II. A structural based model for anisotropic mechanical behaviour of the tissue. *Biomaterials*, 15:374–382, 1994.
45. K. L. Billiar and M. S. Sacks. Biaxial mechanical properties of the fresh and glutaraldehyde treated porcine aortic valve: Part 2. A structurally guided constitutive model. *Journal of Biomechanical Engineering*, 122:327–335, 2000.
46. S. M. Sacks. A structural constitutive model for chemically treated planar tissues under biaxial loading. *Computational Mechanics*, 26:243–249, 2000.
47. S. M. Sacks. Incorporation of sals-derived fiber orientation data into a structural constitutive model for planar collagenous tissues. *Journal of Biomechanical Engineering*, 25:280–287, 2003.
48. M. S. Sacks, D. B. Smith, and E. D. Hiester. A small angle light scattering device for planar connective tissue microstructural analysis. *Annals of Biomedical Engineering*, 25:678–689, 1997.
49. R. D. Crowninshield and M. H. Pope. The strength and failure characteristics of rat medial collateral ligaments. *The Journal of Trauma*, 2:99–105, 1976.
50. C. Lydon, J. J. Crisco, M. Panjabi, and M. Galloway. Effects of elongation rate on the failure properties of the rabbit anterior cruciate ligament. *Clinical Biomechanics*, 10:428–433, 1995.
51. R. C. Haut and R. W. Little. Rheological properties of canine anterior cruciate ligaments. *Journal of Biomechanics*, 2:289–298, 1969.
52. J. J. Crisco, D. C. Moore, and R. D. McGovern. Strain-rate sensitivity of the rabbit mcl diminishes at traumatic loading rates. *Journal of Biomechanics*, 35:1379–1385, 2002.

53. C. E. Jamison, R. D. Marangoni, and A. A. Glaser. Viscoelastic properties of soft tissue by discrete model characterization. *Journal of Biomechanics*, 1:33–46, 1968.
54. R. Sanjeevi. A viscoelastic model for the mechanical properties of biological materials. *Journal of Biomechanics*, 15:107–109, 1982.
55. R. C. Haut and R. W. Little. A constitutive equation for collagen fibers. *Journal of Biomechanics*, 5:423–430, 1972.
56. G. Limbert and Middleton J. A transversely isotropic viscohyperelastic material: Application to the modeling of biological soft connective tissues. *International Journal of Solids and Structures*, 41:4237–4260, 2004.
57. W. Noll. A mathematical theory of the mechanical behavior of continuous media. *Archives in Rational and Mechanical Analysis*, 2:199–226, 1958.
58. P. Flaud and D. Quemada. A structural viscoelastic model for soft tissues. *Biorheology*, 25:95–105, 1988.
59. C. Hurschler, B. Loitz-Ramage, and R. Vanderby. A structurally based stress-stretch relationship for tendon and ligament. *Journal of Biomechanical Engineering*, 119:392–399, 1997.
60. N. Sasaki and S. Odajima. Stress-strain curve and Young’s modulus of a collagen molecule as determined by x-ray diffraction technique. *Journal of Biomechanics*, 29:655–658, 1996.
61. F. H. M. Nestler, S. Hvidt, and J. D. Ferry. Flexibility of collagen determined from dilute solution viscoelastic measurements. *Biopolymers*, 22:1747–1758, 1983.
62. R. W. Ogden. *Non-linear elastic deformations*. Dover, 1997.
63. J. Beck and K. Arnold. *Parameter Estimation in Engineering and Science*. Wiley, New York, 1977.
64. S. M. Belkoff and R. C. Haut. A structural model used to evaluate the changing microstructure of maturing rat skin. *Journal of Biomechanics*, 24:711–720, 1991.
65. C. Hurschler, P. P. Provenzano, and R. Vanderby. Application of a probabilistic microstructural model to determine reference length and toe-to-linear region transition in fibrous connective tissue. *Journal of Biomechanics*, 125:415–422, 2003.
66. H. Liao and S. M. Belkoff. A failure model for ligaments. *Journal of Biomechanics*, 32:183–188, 1999.
67. M. S. Sacks and X. Lin. Extension of sals to transmural quantitative structural analysis of planar tissue. In *Proceedings of Optical Diagnostics of Living Cells II*, San Jose, California, 1999.

68. M. L. Hull, G. S. Berns, and Varma H. Strain in the medial collateral ligament of the human knee under single and combined loads. *Journal of Biomechanics*, 29:199–206, 1996.
69. J. C. Gardiner, J. A. Weiss, and T. D. Rosenberg. Strain in the human medial collateral ligament during valgus loading of the knee. *Clinical Orthopaedics and Related Research*, 391:266–274, 2001.
70. M. K. Kwan and S. L. Y. Woo. A structural model to describe the nonlinear stress-strain behavior for parallel-fibered collagenous tissues. *Journal of Biomechanical Engineering*, 111:361–363, 1989.
71. T. A. L. Wren and D. R. Carter. A microstructural model for the tensile constitutive and failure behavior of soft skeletal connective tissues. *Journal of Biomechanical Engineering*, 120:55–61, 1998.
72. S. K. Park and K. W. Miller. Random number generators: Good ones are hard to find. *Communications of the ACM*, 31:1192–1201, 1988.
73. W. H. Press, B. P. Flannery, S. A. Teukolsky, and W. T. Vetterling. *Numerical Recipes in C: The Art of Scientific Computing*. Cambridge University Press, Cambridge, 1992.
74. J. Nelder and R. Mead. A simplex method for function minimization. *Computer Journal*, 7:308–313, 1965.
75. S. D. Abramowitch, C. D. Papageorgiou, R. E. Debski, T. D. Clineff, and S. L. Y. Woo. A biomechanical and histological evaluation of the structure and function of the healing medial collateral ligament in a goat model. *Knee Surgery, Sports Traumatology, Arthroscopy*, 11:155–162, 2003.
76. P. P. Provenzano, D. Heisey, K. Hayashi, R. Lakes, and Jr. R. Vanderby. Subfailure damage in ligament: a structural and cellular evaluation. *Journal of Applied Physiology*, 92:362–371, 2002.
77. U. Kukreti and S. M. Belkoff. Collagen fibril D-period may change as a function of strain and location in ligament. *Journal of Biomechanics*, 33:1569–1574, 2000.
78. T. Andriacchi, P. Sabiston, K. De Haven, L. Dahners, S. Woo, C. Frank, B. Oakes, R. Brand, and J. Lewis. Ligament: injury and repair. In S. Y. L. Woo and J. A. Buckwalter, editors, *Injury and Repair of the Musculoskeletal Soft Tissues*. AAOS, Park Ridge, IL, 1987.
79. G. Laws and M. Walton. Fibroblastic healing of grade ii ligament injuries. histological and mechanical studies in the sheep. *Journal of Bone and Joint Surgery - British Volume*, 70:390–396, 1988.
80. M. M. Panjabi, E. Yoldas, T. R. Oxland, and J. J. Crisco III. Subfailure injury of the rabbit anterior cruciate ligament. *Journal of Orthopaedic Research*, 14:216–222, 1996.

81. P. F. Davison. The contribution of labile crosslinks to the tensile behavior of tendons. *Connective Tissue Research*, 18:293–305, 1989.
82. P. Fratzl, K. Misof, I. Zizak, G. Rapp, H. Amenitsch, and S. Bernstorff. Fibrillar structure and mechanical properties of collagen. *Journal of Structural Biology*, 122:119–122, 1997.